

SIMULATING THE EFFECTS OF PRESCRIBED FIRE ON FORESTED LANDSCAPES IN
THE SISKIYOU MOUNTAINS, USA

BY

ALISON DEAK

A THESIS

Presented to the Department of Geography
and the Division of Graduate Studies of the University of Oregon

in partial fulfillment of the requirements

for the degree of

Master of Science

September 2022

THESIS APPROVAL PAGE

Student: Alison Deak

Title: Simulating the Effects of Prescribed Fire on Forested Landscapes in the Siskiyou Mountains,
USA

This thesis has been accepted and approved in partial fulfillment of the requirements for the Master of
Science degree in the Department of Geography by:

Dr. Lucas Silva Geography

Dr. Melissa Lucash Geography

Dr. Michael Coughlan Institute for Resilient Organizations, Communities, and Environments

and

Krista Chronister Vice Provost for Graduate Studies

Original approval signatures are on file with the University of Oregon Division of Graduate Studies.

Degree awarded September 2022

© 2022 Alison Deak

THESIS ABSTRACT

Alison Deak

Master of Science

Department of Geography

September 2022

Title: Simulating the Effects of Prescribed Fire on Forested Landscapes, Siskiyou Mountains, USA

Land managers, scientists, and policymakers have increasingly promoted and invested in prescribed fire to reduce wildfire risk and restore fire-adapted ecosystems. We investigate the amount of prescribed fire needed to meet these goals in the Siskiyou Mountains of northwest California and southwest Oregon using a forest-succession model. Specifically, we ask, how much prescribed fire is required to maintain carbon storage and reduce the severity and extent of wildfires under divergent climate change scenarios?

A prescribed fire frequency of fifteen years was found adequate for maintaining carbon storage on sites. Prescribed fire lowered the severity of wildfires at a local-scale and was most effective under a warmer and wetter climate. These results suggest targeting treatments in areas with high social-ecological concern and within climactic and topographic gradients most conducive to its effects will provide opportunities to decrease the risk of high-severity fire and contribute to meeting climate mitigation goals.

CURRICULUM VITAE

NAME OF AUTHOR: Alison Deak

GRADUATE AND UNDERGRADUATE SCHOOLS ATTENDED:

University of Oregon, Eugene
University of Colorado Colorado Springs, Colorado Springs

DEGREES AWARDED:

Master of Science, Geography, 2022, University of Oregon
Master of Nonprofit Management, 2021, University of Oregon
Bachelor of Arts, Geography and Environmental Studies, University of Colorado Colorado Springs

AREAS OF SPECIAL INTEREST:

Pyrogeography
Human-Environmental Interactions

PROFESSIONAL EXPERIENCE:

Research Assistant, Ecosystem Workforce Program, Institute for Resilient Organizations, Communities, and Environments, University of Oregon, 2019-2022
Teaching Assistant, Geography Department, University of Oregon, 2020-2021

GRANTS, AWARDS, AND HONORS:

College of Design Scholarship, University of Oregon, 2020
David S. Easley Graduate Scholarship, University of Oregon, 2020
Nonprofit Sector Research Fund, University of Oregon, 2020
Kantor Family Internship Scholarship, University of Oregon, 2020
Cum Laude, University of Colorado Colorado Springs, 2015
Dane M. Vogel Scholarship, University of Colorado Colorado Springs, 2014
Jacquelyn Beyer Fellowship, University of Colorado Colorado Springs, 2014
Boundless Opportunity Scholarship, University of Colorado Colorado Springs, 2014

PUBLICATIONS:

- Davis, E. J., Huber-Stearns, H., Caggiano, M., McAvoy, D., Cheng, A. S., Deak, A., & Evans, A. (2022). Managed Wildfire: A Strategy Facilitated by Civil Society Partnerships and Interagency Cooperation. *Society & Natural Resources*, 1-19.
- Jacobson, M., Smith, H., Huber-Stearns, H. R., Davis, E. J., Cheng, A. S., & Deak, A. (2021). Comparing social constructions of wildfire risk across media, government, and participatory discourse in a Colorado fireshed. *Journal of Risk Research*, 1-18.

ACKNOWLEDGMENTS

I am overwhelmed by gratitude for the enormous generosity and contributions of mentors, colleagues, family, and friends that have made this research possible.

I first wish to express gratitude to Dr. Lucas Silva. Through his contagious love of science and encouragement to pursue fire-related questions, he has been pivotal in my life by helping me discover a passion for fire science. His patience, support, and guidance were vital for writing this story.

Dr. Melissa Lucash has been a mentor and a friend. Her generosity with time and wealth of knowledge has made this research possible. She provided me with a community by welcoming me into her lab and her words of encouragement gave me the confidence I needed to continue when I didn't know how.

Dr. Michael Coughlan's mentorship and passion for Indigenous traditional knowledge took this research on some unexpected paths and led me to expand my worldview. He has been a mentor, a colleague, and a friend; I am grateful to him for making me a better and more well-rounded scientist and writer.

The unwavering support and mentorship of Dr. Heidi Huber-Stearns has been formative in the direction of this research and my evolution as a scientist. Through the countless opportunities she has provided me, she has given me the courage and skillsets that have allowed me to pursue new chapters in my life that I never dreamed possible.

The Soil-Plant-Atmosphere Lab has been a continual source of inspiration for their rigorous pursuit of scientific knowledge. I want to especially thank Hilary Rose Dawson for her insight, knowledge, and friendship and Sydney Katz for being a friend and dependable source of a good laugh. I also want to thank Hilary Rose, Sydney, Dr. Lucas Silva, Ori Chafe, Adrianna Uscanga-Castillo, Jamie Wright, and Delaney Kleiner for their help with fieldwork in the Siskiyou Mountains.

The Terrestrial Ecosystem Ecology and Landscapes Lab has been instrumental in this research by sharing their intellectual knowledge and friendship. Shelby Weiss spent innumerable hours guiding me through the modeling process, never hesitated to share her scripts, and helped me think through much of this research. James Lamping's infectious positivity and countless conversations over beers and trail runs has helped make research a whole lot more fun. I also thank Dr. Thomas Brussel and Dr. Neil Williams for their guidance and for sharing their time and experience.

I am grateful to my family for their support and understanding as I've pursued graduate school. I thank my father, George Deak, for always reminding me how smart I am even when I'm not acting particularly smart. I thank my mother, Wendy Lewis, for always being my biggest supporter and for believing in me when I don't believe in myself. I thank my sister, Jessica Deak, for being a friend, confidant, and co-conspirator on the move to Oregon.

Finally, I am filled with gratitude and wonder for Zachary Higgins' steadfast love and support while I've pursued two graduate degrees. I could never have imagined a better partner and best friend. Thank you for taking this journey with me.

TABLE OF CONTENTS

I. INTRODUCTION	1
II. METHODOLOGY	6
Study area	6
Overview of simulation model	7
Model parameterization validation, and calibration	9
Climate regions	10
Simulated climate scenarios	10
Initial vegetative communities	12
Soils	13
Fire	14
Timber harvesting	17
Scenarios	17
Analysis	17
Landscape-scale analyses	18
Local-scale analyses	19
III. RESULTS	20
Landscape-scale	20
Local-scale	23
IV. DISCUSSION	27
Limitations	28
V. CONCLUSION	30
APPENDICES	32

A. Climate region classification	32
B. Species simulated	33
C. Tree and shrub ages	34
D. Aboveground carbon storage	35
E. NECN species parameterization	36
F. Validation of LANDIS-II initial communities map	39
G. SCRPPLE fire calibration	42
H. Timber harvest scenarios	43
REFERENCES CITED	44

LIST OF FIGURES

1.	Theoretical relationship between carbon storage and carbon stability.	4
2.	Study landscape	6
3.	Average aboveground carbon consumed by ignition type during the 50-year simulations across climate and treatment scenarios	20
4.	Change in mean severity, as measured by dNBR, of wildfires for each simulation year across treatment and climate scenarios	21
5.	Change in mean burn severity between the first and last 25 years of the simulation by treatment scenario	22
6.	The distributions of area burned by the largest 25 percent of wildfires across treatment and climate scenarios	23
7.	Mean aboveground and soil organic carbon storage of cells with increasingly prescribed fire treatment frequency across climate scenarios	25
8.	Effects of prescribed fire on wildfire severity	26

LIST OF TABLES

1.	Sources used to parameterize inputs to model	9
2a.	Average annual precipitation, maximum daily temperature, and minimum daily temperature in the historical climate scenario for each climate region	11
2b.	Change in annual precipitation, average maximum daily temperature, and average minimum daily temperature in the climate change scenarios for each climate region	12
3.	Treatment scenarios simulated across climate scenarios	17

CHAPTER I.

INTRODUCTION

Consensus amongst land managers and scientists continues to converge on the need to increase the use of prescribed fires, or fires set intentionally to achieve treatment objectives, to restore fire-adapted ecosystems and reduce wildfire risk (Kolden, 2019; Levy, 2022; Schultz et al., 2019; Stephens et al., 2020; A. H. Taylor et al., 2021). Meanwhile, Indigenous communities are increasingly asserting their sovereignty and traditions by revitalizing cultural burning practices (Adlam et al., 2021; Lake et al., 2017; Marks-Block & Tripp, 2021). As more partnerships form between land managers, tribes, and other stakeholders to restore fire-adapted ecosystems and manage wildfire risk (Davis et al., 2021; Lake, 2021), a key question remains: how much prescribed fire do land managers need to be implementing to meet these goals, especially given climate change? Specifically, we ask, what prescribed frequency or extent of prescribed fire is needed to maintain carbon stores on the landscape and reduce the severity and extent of wildfires under divergent climate change scenarios?

This question is particularly important to ask for landscapes with mixed-severity fire regimes because they are the most widespread, yet challenging, for scientists and managers in the western US to understand (Agee, 2005; Halofsky et al., 2011; Schoennagel et al., 2004). Mixed severity fire regimes are those that experience a spectrum from low to high fire severity effects. Forests with mixed-severity fire regimes are adapted to small and frequent fires that leave behind heterogeneous patchworks of forest at various stages of the successional process. In the past, fires burning across this patchwork were influenced not only by fuels, topography, and weather, but also by differences in vegetative composition and structure within a mosaic of patches created by previous fires (Agee,

1993; Halofsky et al., 2011). The heterogeneity created by these uneven burning patterns is strongly related to ecosystem structure and function and plays a crucial role in the sustainability and resiliency of ecosystems (Perry et al., 2011; Turner et al., 2013).

The Siskiyou Mountains of northwest California and southwest Oregon, and the larger Klamath Mountains ecoregion, are a hub for research aimed at understanding mixed-severity fire regimes (Donato et al., 2009; Halofsky et al., 2011) and the potential for vegetative shifts driven by climate change and altered fire regimes (Damschen et al., 2010; Serra-Diaz et al., 2018; Tepley et al., 2017). The Siskiyou Mountains are a biodiverse landscape with a rich history of fire, having been actively stewarded by Indigenous peoples using cultural burning practices for millennia prior to Euro-American settlement (Knight et al., 2022). It is well understood that through these practices, Indigenous peoples lowered stand densities and helped maintain the old growth characteristics of forests (Agee, 1993), reduced fire hazard and the buildup of fuels (Sensenig et al., 2013; Long et al., 2021), and maintained a diversity of habitats (Kimmerer & Lake, 2001; Lewis, 1973). The average fire return interval was between eight and 20 years with most fires occurring in spring and fall until the late 1800s when Euro-American settlement disrupted pre-settlement fire regimes (Knight et al., 2022; Metlen et al., 2018; A. H. Taylor & Skinner, 2003).

By the end of the 19th century many Indigenous groups had been displaced and the United States Forest Service (USFS) effectively eliminated any remaining Indigenous cultural burning beginning in 1910 with a campaign to eliminate fires set by those residing in the area (LaLande & Pullen, 1999, p. 260). Other fires on the landscape were also suppressed through policies such as the 10 AM policy of 1935 which mandated that all fires be extinguished by 10 AM the day after being reported (Pyne, 1997). Despite widespread consensus that forests would benefit from increased low- to moderate-severity fire (Kolden, 2019), the USFS continues to suppress and rapidly contain nearly 98% of wildfires (USFS, 2015). By doing so, federal fire managers are “preferentially selecting for

more damaging fires that burn under more extreme conditions” (Dunn et al., 2020). Consequently, the dry forests of the Pacific Northwest adapted to frequent low- to mixed-severity fire are experiencing a “fire deficit” (Haugo et al., 2019; Marlon et al., 2012). When fires do burn in this landscape, they are larger and more severe than the estimated historic range of variation due to fuels buildup and climate change (Haugo et al., 2019; Parks & Abatzoglou, 2020) leading to drastic effects on long-term carbon storage.

Although fire suppression has increased the United States’ aboveground carbon stores during the 20th century, carbon sequestration is expected to decline over the 21st century (Hurtt et al., 2002) as a result of increased difficulty suppressing larger and more severe wildfires. This is concerning because forests in the Pacific Northwest have enormous carbon sequestration potential due to their longevity and high productivity (Hudiburg et al., 2009; Smithwick et al., 2002). Frequent, low-severity fires through prescribed fire, cultural burning, and wildland fires managed for resource benefits (i.e., managed fires) alongside thinning treatments reduce severity and spread rate of subsequent fires, decrease extreme fire behavior by reducing the loading and continuity of fuels available to burn (Cochrane et al., 2012; Fernandes, 2015), decrease tree mortality (Kalies & Kent, 2016), and sustain ecosystem services, such as carbon sequestration.

Carbon stabilization, or the maintenance of carbon stocks through time, reduces the risk of carbon being returned to the atmosphere through combustion during fire events (Hurteau et al., 2019; Hurteau & Brooks, 2011). Although carbon storage may be immediately lowered following a prescribed burn operation where younger trees are killed, older trees storing larger amounts of carbon are more likely to survive in burned areas that have been treated. This results in a net increase of carbon over time that is less prone to high-severity fire due to decreased fuel loads and therefore, less likely to convert to a less productive or non-forested state following a high-severity event (Figure 1; Hurteau et al., 2019; Hurteau & Brooks, 2011). Although Hurteau and Brooks

(2011) only define carbon stabilization to include aboveground carbon, soil organic carbon is also at increased risk of combustion from the accumulation of fuel loads (Pellegrini et al., 2018; Restaino & Peterson, 2013; Zhou et al., 2022). Therefore, this definition of carbon stabilization has been expanded to include the maintenance of both aboveground and soil organic carbon stocks through time.

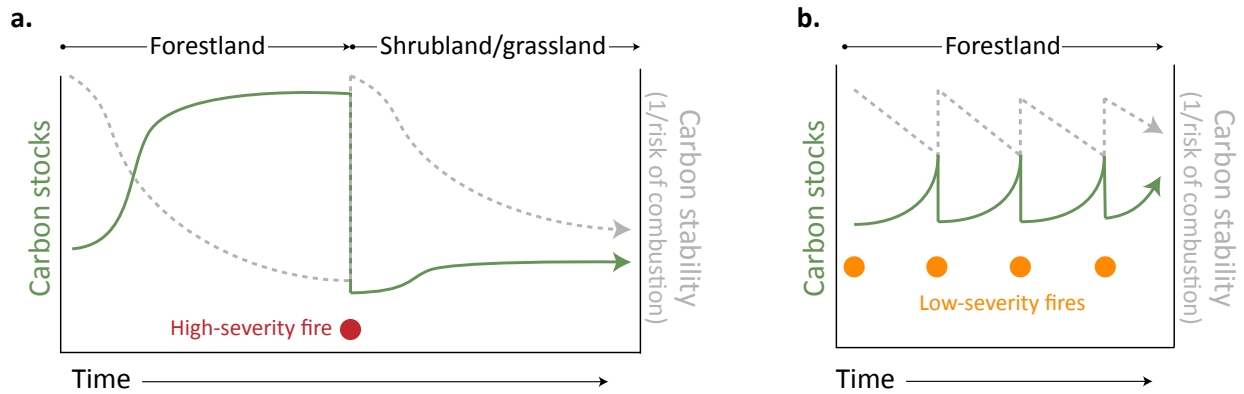


Figure 1. Theoretical relationship between carbon storage and carbon stability, i.e., the maintenance of carbon stocks through time. (a) Fire suppression increases carbon storage but increases the potential for combustion during high-severity fire events which can deplete carbon storage and convert forest to a shrubland or grassland, reducing its long-term potential for carbon storage. (b) Frequent low-severity fire from prescribed fires, reduces short-term carbon storage but reduces the risk of carbon loss due to lowered risk of combustion and therefore promotes carbon stability. Adapted from Hurteau & Brooks (2011).

While the use of prescribed fire to maintain ecosystem services, restore fire-adapted ecosystems, and manage wildfire risk is promising, current fuels mitigation treatments have not reached the pace and scale needed to do so (Kolden, 2019; Vaillant & Reinhardt, 2017). However, this is rapidly changing. With the United States’ passage of the 2021 Infrastructure Investment and Jobs Act, billions of additional dollars are being invested towards land management over the next decade. The 2022 USFS Wildfire Crisis Strategy aims to treat an additional 8 million hectares (20 million acres) of National Forest lands and over 12 million hectares (30 million acres) of other Federal, State, Tribal, and private lands. Strategically investing these funds and positioning

treatments will be critical for addressing wildfire risk to ecosystems and communities across the nation.

Landscape simulation models offer a powerful way for managers to elucidate the amount of fire at different scales required to meet these ambitious treatment goals in various landscapes and experiment with different treatment frequencies and extents on landscapes. Through this paper, we demonstrate how increasing prescribed fire frequency and extent within a landscape can alter the trajectory of future fire regimes and stabilize carbon stocks in the Siskiyou Mountains under climate change. We analyzed changes in aboveground and soil organic carbon storage at a local-scale (simulated as 30-meter landscape cells) and fire regime attributes at the landscape scale by testing the following hypotheses: (1) cells with increased prescribed fire frequency will have lower yet more stable aboveground and soil organic carbon storage in all climate scenarios due to lowered carbon consumption during wildfire events; (2) the severity of wildland fires occurring on the study landscape will decrease with increased prescribed fire frequency and extent in all climate scenarios; and (3) The median size of the largest wildland fires on the study landscape will decrease with increasing prescribed fire frequency and extent in all climate scenarios.

CHAPTER II.
METHODOLOGY

Study area

The study area comprises 171,179 hectares within the Siskiyou Mountains known as the “Serpentine Siskiyou” for their distinct nutrient-poor serpentine soils (Griffith et al., 2016). The Siskiyou Mountains are the northernmost range of the larger Klamath Mountains ecoregion and extend in an east-west direction along the California-Oregon border between the Coast and Cascade Ranges. (Figure 1a and 1b). Elevation in the study area ranges from 27–1620 m above sea level (USGS, 2020).

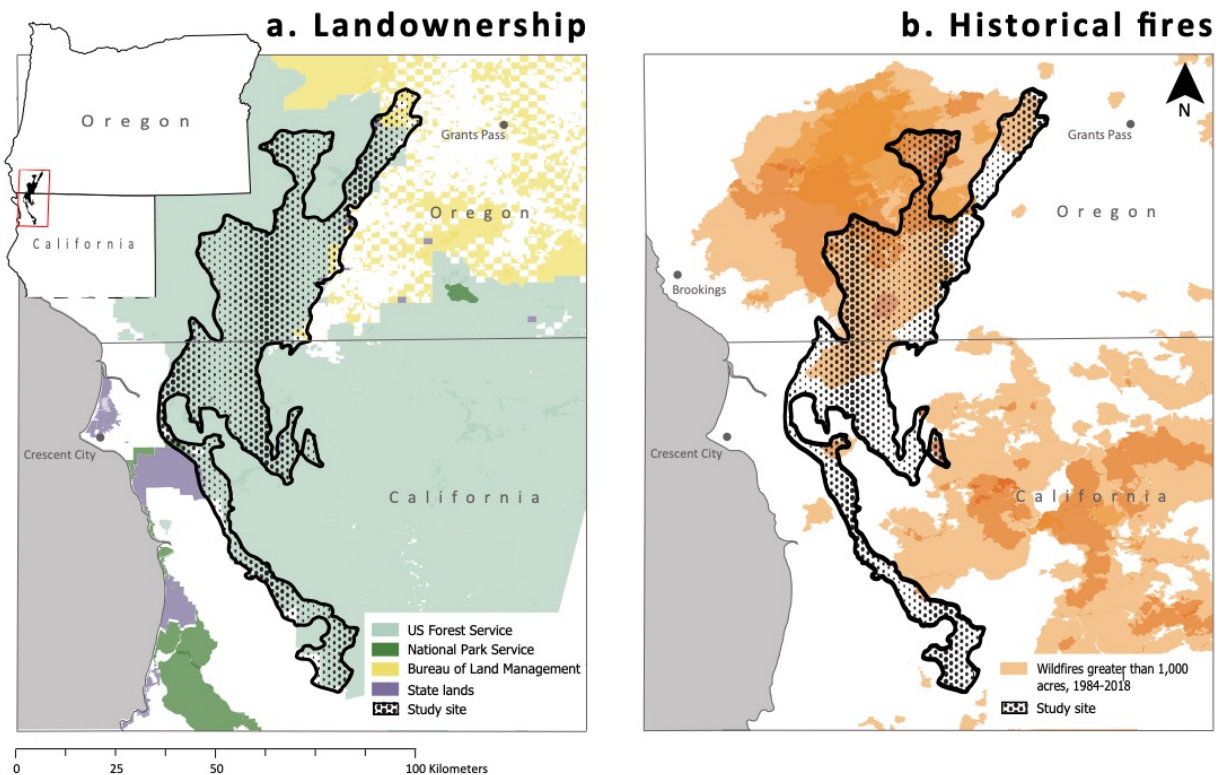


Figure 2. Study landscape. (a) Landownership of the study area and surrounding area. Data source: USGS Gap Analysis Project (2018). (b) Wildfires greater than 1,000 acres in size occurring across the study area between 1984 and 2018. Reburn areas are indicated by a darker hue on the map. Data source: USFS & USGS (2018)

Vegetation in the Siskiyou Mountains is exceptionally diverse due to elevational and climatic gradients, soil parent materials, and mixed-severity fire regime, with a heterogeneous mixture of conifer and hardwood forests, shrublands, and prairies of perennial grasses and oak woodlands being present throughout (Agee, 1991; Whittaker, 1960). In the serpentine Siskiyou, Douglas fir (*Pseudotsuga mensiezi*) and western white pine (*Pinus monticola*) are common and Jeffrey Pine (*Pinus Jeffreyi*), endemic oak species (*Quercus spp.*), ceanothus species (*ceanothus spp.*), and many forb species have evolved to grow in the nutrient poor soils.

The study area is characterized by a Mediterranean climate with long, hot summers and cool, wet winters (Whittaker, 1960). Mean minimum January and maximum June temperatures across the study area are 1.7°C and 28.9 °C, respectively, with an average annual precipitation of 1,803 mm (1991-2020; NCEI, 2020).

The study area is currently managed primarily by the Rogue River and Six Rivers National Forests (91.4%) with a small portion of the remaining landscape falling within private land ownership (8.3%) and management by the Bureau of Land Management (1.2%) and Oregon and California state parks and recreation departments (0.1%, Figure 1b). This landscape is the ancestral homeland of and was traditionally managed by the Chetco, Coquille, Cow Creek Band of Umpqua, Karuk, Shasta, Takelma, Tolowa Dee-ni', Tututni, and Yurok peoples.

Overview of simulation model

Using the raster-based dynamic forest landscape change model LANDIS-II (Scheller et al., 2007), we simulated changes in biomass and fire regimes. This model has been widely used to simulate forest succession and response to disturbance, treatment, and climate change scenarios in the western U.S. (Cassell et al., 2019; Duveneck et al., 2014; Liang et al., 2018; Serra-Diaz et al., 2018; Syphard et al., 2011). We chose the LANDIS-II modeling framework due to its ability to

simultaneously simulate the effects of climate change and disturbance on forest succession at a landscape-scale over long-time periods.

LANDIS-II uses species' life history attributes to simulate vegetation change driven by disturbance and succession (Mladenoff, 2004; Scheller et al., 2007). LANDIS-II simulates species-age cohorts, meaning species are discretely grouped into user-specified age bins that are altered simultaneously by disturbance, succession, and management. Each species is parameterized with its own life history attributes, such as shade and fire tolerance, longevity, and seed dispersal ability, and is responsive to changes in climate due to optimal temperature ranges and drought tolerance. Processes, such as competition, growth, and mortality are simulated independently for each species-age cohort within each site, while other processes, such as fire and seed dispersal, are simulated both within and across sites.

We used the LANDIS-II core v7 with the Net Ecosystem Carbon and Nitrogen (NECN) succession extension v6.9 (Scheller et al., 2011) to simulate forest growth, reproduction, and mortality. NECN tracks above and belowground carbon and nitrogen pools and fluxes while limiting cohort growth based on leaf area index, soil water availability, temperature, growing space capacity, and nitrogen availability at monthly timesteps (Lucash et al., 2018; Scheller et al., 2011). Weather inputs to NECN include temperature, precipitation, relative humidity, and wind speed and direction. We used the Biomass Output extension to obtain total aboveground biomass for each species at 10-year timesteps (Scheller & Mladenoff, 2004).

Both fire and forest management were simulated across the landscape. The Social-Climate Related Pyrogenic Processes and their Landscape Effects (SCRPPLE) v3.2 extension was used to simulate natural, human-accidental, and prescribed fire (Scheller et al., 2019). Fire spread and species mortality resulting from fire is based on user-defined inputs and algorithms in the model dictating ignition, intensity, and suppression for each of the three types of wildland fire. At daily time steps,

the probability of ignition, spread, and mortality is calculated for each cell based on fire weather index, topography, and vegetation dynamics. To simulate forest harvest and management, we used the Biomass Harvest extension v4.4 (Gustafson et al., 2000). This extension simulates the removal of biomass through harvesting activities and the replanting of species following harvest. User-defined prescriptions dictate the amount of biomass removed from specified species-age cohorts within forest stands. The Dynamic Biomass Fuels Extension v3.0.1 was used to determine fuel types and amounts across the landscape (Syphard et al., 2011). This extension is required by the biomass harvest extension to inform where harvest occurs on the landscape based on fuel loads.

Model parameterization, validation, and calibration

All R scripts used to parameterize, validate, and calibrate model inputs are publicly available on the LANDIS-II Foundation GitHub page (<https://github.com/LANDIS-II-Foundation>). Data sources used to parameterize model inputs and perform calibration are included in Table 1.

Table 1. Sources used to parameterize inputs to model.

Extension	Parameter	Data sources
Climate library	Climate regions	Abatzoglou & Brown (2012)
	Climate scenarios	PRISM Climate Group (2021)
	Species	Fire Effects Information System (https://www.feis-crs.org/feis/#) North American Silvics Manual (Burns & Honkala, 1990) Long et al. (2018) TRY plant trait database (Kattge et al., 2020) USGS Vegetation Atlas of North America (Thompson et al., 2006) Loudermilk et al. (2014) Serra-Diaz et al. (2018)
Forest succession (NECN)	Functional groups	See Appendix E for full list
	Initial communities	Forest Inventory & Analysis (USFS, 2021) LEMMA (Ohmann & Gregory, 2002) Woodall et al. (2010) Keyser (2019) Riccardi et al (2007)

Table 1, continued

Extension	Parameter	Data sources
Fire (SCRPPLE)	Soils	Soil Web (Walkinshaw et al., 2020) STATSGO (Schwarz & Alexander, 1995) Wilson et al. (2013) West (2014) Forest Inventory & Analysis (USFS, 2021)
	Suppression	1/3-arc second resolution Digital Elevation Model (USGS, 2020) Roads (US Census Bureau, 2001) WUI data (Radeloff et al., 2018) Wilderness areas (Wilderness Connect, 2021)
	Spread	1/3-arc second resolution Digital elevation models (USGS, 2020) Abatzoglou (2013) LANDFIRE (2014)
	Severity	Monitoring Trends in Burn Severity (USFS & USGS, 2021)
	Ignitions	Short (2021)
	Prescribed fire	National Fire Plan Operations Reporting System (USGS, 2021)
	Species mortality	Fire and Tree Mortality Database (Cansler et al., 2020) First Order Fire Effects Severity Model (Hood & Lute, 2017)
Biomass harvest	Harvest scenarios	Maxwell et al (2020)

Climate regions

NECN requires grouping cells throughout the study landscape into homogenous climate regions. Three climate regions were delineated for the study landscape based on 30-year average (1991-2020) precipitation, maximum temperature, and minimum temperature values for months during the growing season (i.e., months with an average temperature greater than 5°C) at 4-km resolution from the PRISM Climate Group (2021). Unsupervised classification using K-means clustering and Clustering Large Applications (CLARA) delineated three climate regions on the study landscape; the K-means clustering analysis produced a larger silhouette index (i.e., measurement of how well clusters have been classified) indicating better overall performance. The output from this analysis was used to generate climate regions from which homogenous daily weather is simulated (See

Appendix A for workflow).

Simulated climate scenarios

Daily historical and future weather data based on climate change scenarios were retrieved from the USGS Geodata Portal (<https://cida.usgs.gov/gdp/>) for each of the three climate regions. For climate scenarios, we used statistically downscaled global climate model (GCM) data from CMIP5 (K. E. Taylor et al., 2012) utilizing a modification of the Multivariate Adaptive Constructed Analogs method (Abatzoglou & Brown, 2012). Predicted daily precipitation (mm), minimum and maximum relative humidity (%), maximum near-surface air temperature (K), windspeed (m/s), and wind direction were obtained using area weighted grid statistics for each of the three climate regions. We selected the CNRM-CM5 climate model to represent historical data (1950-2005) due to its availability through the USGS Geodata Portal and its strong predictive performance in the Pacific Northwest (Rupp et al., 2013). To simulate historical climate, annual data were randomly selected during each year of the simulation (Table 2a). We simulated two high-emissions climate models to capture the spectrum of predicted climate change across the climate regions identified on the landscape for the period 2020-2070. The first represents a large increase in annual precipitation with a moderate increase in temperature (henceforth, the “warmer and wetter” scenario). The second represents a large decrease in precipitation with a larger increase in temperature (henceforth, the “warmer and drier” scenario; Table 2b).

Table 2a. Average annual precipitation, maximum daily temperature, minimum daily temperature in the contemporary climate scenario for each climate region.

Climate scenario (CMIP5 climate model)	Climate region	Annual precipitation	Average maximum temperature	Average minimum temperature
Contemporary (1950-2005) (CNRM-CM5)	1	160 mm	18.4°C	4.9°C
	2	267 mm	17.7°C	5.6°C
	3	340 mm	17.1°C	5.0°C

Table 2b. Change in annual precipitation, average maximum daily temperature, and average minimum daily temperature in the climate change scenarios for each climate region. Changes in precipitation and temperature for climate change scenarios are the difference between the five-year averages of temperature variables at the beginning (2020-2025) and end (2065-2070) of the simulated climate change scenarios.

Climate scenario (CMIP5 climate model)	Climate region	Change in annual precipitation	Change in average maximum temperature	Change in average minimum temperature
Warmer & drier (GCM8.5 MIROC-ESM-CHEM)	1	-57 mm	+4.1°C	+3.5°C
	2	-95 mm	+3.4°C	+3.0°C
	3	-123 mm	+4.0°C	+3.4°C
Warmer & wetter (GCM8.5 CNRM-CM5)	1	+40 mm	+2.8°C	+3.0°C
	2	+59 mm	+2.3°C	+2.5°C
	3	+77 mm	+2.6°C	+2.8°C

Initial vegetative communities

To develop initial vegetative communities, we interpolated USFS Service Forest Inventory and Analysis (FIA) data (USFS, 2022) based on gradient nearest neighbor (GNN) maps developed by the Landscape Ecology, Modeling, and Mapping Analysis (LEMMA) group (Ohmann & Gregory, 2002). 30-meter resolution species distribution, stand age, and forest type raster data from LEMMA were masked to the study landscape extent and FIA plots were iteratively assigned to each cell based on whether species composition, forest type, and/or stand age within FIA plots matched the LEMMA GNN maps. Sequential map codes were then assigned for each unique FIA plot. Cells designated as developed, industrial, open water, and agricultural were made inactive. A total of 666 unique vegetative communities were distributed across the study area.

Shrub species grouped by genus and tree species identified within greater than 10% of FIA plots within the defined study landscape were simulated (see Appendix B for full list of species simulated). Tree ages were computed using the large tree height growth equations from the USFS Forest Vegetation Simulator (Keyser, 2019). Shrub ages were then input into cells based on stand

age from the corresponding FIA plot (See Appendix C). Initial tree biomass was estimated using the component ratio method (Woodall et al, 2011) as used by FIA. Initial shrub biomass was calculated for each shrub functional group using allometric equations from Riccardi et al. (2007) based on plot-level FIA data for species height and cover percent (See Appendix D for aboveground carbon comparisons to FIA-derived aboveground carbon estimates).

Species parameters were obtained from the literature and available datasets. These included the USFS Fire Effects Information System (<https://www.feis-crs.org/feis/>), North American Silvics Manual (Burns & Honkala, 1990), Long et al. (2018), the TRY plant trait database (Kattge et al., 2020), US Geological Survey Vegetation Atlas of North America (Thompson et al., 2006), and from previous studies utilizing LANDIS-II (Loudermilk et al., 2014; Serra-Diaz et al., 2018). (The sources used to parameterize functional group parameters are available in Appendix E.)

We validated initial communities across the landscape by comparing the distributions of each cell of the simulated landscape's leaf area index (LAI) during June of the first time step to the MODIS Level-4 LAI product (Myneni & Park, 2015) and LAI values calculated from the ICESat-2 ATL03 product (Neumann et al, 2021) using methods by Zhang et al. (2021). LAI is a unitless measurement of canopy foliage considered to be a reliable proxy for aboveground net primary productivity (Asner et al., 2003). Although LAI values at each cell showed poor agreement with both MODIS and ICESat-2 derived values, the distribution of LAI values fell within the range of values expected by these datasets (for more information see Appendix F).

Soils

NECN requires soil inputs to simulate forest succession and calculate species growth within cells. Soil depth, drainage class, percent sand, and percent clay data were acquired from the UCDavis SoilWeb application (Walkinshaw et al., 2020). The UCDavis SoilWeb application aggregates current

US Department of Agriculture Natural Resource Conservation Service soil survey data across all soil layers within 800-m grid cells. These data were manipulated to the correct NECN parameters, coordinate reference system, extent, and resolution then masked to the study landscape. Soil carbon and nitrogen was calculated based on soil carbon estimates in 20-cm layers to 1-meter depth from the Oak Ridge National Laboratory Distributed Active Archive Center for Biogeochemical Dynamics (West, 2014). These data were summed across depths, cropped, reprojected, and calculated to estimate ratios of carbon and nitrogen within each soil pool (Parton et al., 1987, 1988). Field capacity and wilting point data was calculated using STATSGO shapefiles, whereas field capacity is based on the volumetric content of soil water retained at a tension of 1/3 bar and wilting point is the volumetric content of soil water retained at a tension of 15 bars (Schwarz & Alexander, 1995). The initial amount of below ground dead coarse roots were interpolated across the landscape from FIA data (USFS, 2022) based on carbon estimates from coarse roots greater than 0.1 inch in diameter and multiplying by 44% based on the ratio from Mattson and Zhang (2019). Surficial dead woody material was derived from Wilson et al.'s (2013) forest carbon stocks of the contiguous United States (2000-2009).

Fire

We derived lightning, human-accidental, and prescribed fire parameters based on empirical data. Between 1992 and 2018, an average of seven wildfires were ignited within the study area annually, burning an average of 8,243 hectares (Figure 2b). Human-caused ignitions were the most common source of ignition, making up 65% of all ignitions (Short, 2021). Fire was calibrated to closely match annual area burned (mean: 8,243 ha), fire size (mean: 1,239 ha), and average fire severity (50% low, 26% moderate, 24% high) for the period 1992 to 2017 in the study area (see Appendix G; USDA Forest Service & US Geological Survey, 2021).

SCRPPLE calculates differenced Normalized Burn Ratio (dNBR) for each cell on the landscape burned during a fire event; dNBR is a commonly used index calculated from remotely sensed imagery to assess wildfire severity based on changes in the spectral responses of vegetation in burned areas. The severity of wildfires and cells affected by wildfire were categorized using a dNBR threshold for low, moderate, and high severity classes of fires occurring within the study landscape. Fires occurring within a 1-km buffer of the study area from 1984-2019 were subset from the Monitoring Trends in Burn Severity fire occurrence dataset (MTBS; USDA Forest Service & US Geological Survey, 2021b) and analyzed. Each fire in MTBS data has significant burn severity thresholds determined by analysts based on the range of dNBR and Relativized dNBR values found (Eidenshink et al., 2007). dNBR values consistently less than 200 were identified as low severity, between 200 and 439 as moderate severity, and values equal or greater than 440 as high severity.

Kernel density maps of historical ignition locations of lightning and human-accidental ignitions (Short, 2021) were used to determine each cell's probability of ignition. We parameterized maximum suppression to occur on cells within the wildland-urban interface (i.e., zones of transition between the developed and natural environments with higher fire risk), moderate suppression to occur on cells representing roads, and light suppression to occur on cells representing ridgelines. We parameterized the model so that fires ignited by lightning in wilderness areas would not be suppressed.

Fire spread in SCRPPLE is based on an empirical relationship between historical daily fire spread and fire weather index, effective wind speed calculated from slope, uphill slope azimuth, windspeed, wind direction, and fine fuels loading in each cell on the day of fire spread (Scheller et al., 2019). Mortality at the cell is determined based on a relationship between mortality (USDA Forest Service & US Geological Survey, 2021a) and effective wind speed, the previous year's climatic water deficit and actual evapotranspiration (Abatzoglou et al., 2018), fine fuels loading (calculated by

LANDIS-II), and ladder fuels (LANDFIRE, 2014) on the day of spread. Fire severity calculated as dNBR is determined at the scale of the species cohort. Species cohort mortality was derived based on species' bark thickness, a measure used by the model to determine species' susceptibility to mortality at different fire severities; this was parameterized using empirical values from the Fire and Tree Mortality Database (Cansler et al., 2020) and bark thickness coefficients from the First Order Fire Effects Model (Hood & Lutes, 2017) when empirical values were not available.

Prescribed fires were parameterized to burn at the lowest severity class and could occur anywhere outside of wilderness areas. Only one prescribed fire could be ignited each day and only during favorable climatic conditions based on relative humidity, fire weather index, wind speed, and temperature thresholds. Four prescribed fire scenarios were simulated representing (1) no prescribed fire (henceforth the "No-Rx" treatment scenario), (2) business-as-usual, (3) a moderate increase, and (4) a large increase (Table 2). In the business-as-usual treatment scenario ("1x-Rx"), we simulated the mean prescribed fire size and frequency of annual ignitions on the study area between 2002 and 2021. Historical prescribed fire data for the 1x-Rx treatment scenario were derived from the USGS National Fire Plan Operations Reporting System dataset (<https://usgs.nfpors.gov/>) finding an average of five prescribed fires ignited on the landscape annually burning between 1.6 and 54 hectares each. The mean size of prescribed fires on the landscape was 14 hectares (USGS, 2021). For the moderate increase treatment scenario ("3x-Rx") and large increase treatment scenario ("10x-Rx"), the average number and size of prescribed fires were multiplied by three and ten times, respectively (Table 3). We chose the moderate increase scenario to demonstrate how current treatment goals set by the USFS (USDA Forest Service, 2022) may affect the study area and the large increase scenario to ensure the landscape experienced a strong response to prescribed fire.

Table 3. Treatment scenarios simulated across climate scenarios.

Prescribed fire scenario	Number of fires ignited annually	Maximum fire size (hectares)
No prescribed fire (No-Rx)	0	0
Business-as-usual (1x-Rx)	5	14
Moderate increase (3x-Rx)	15	48
Large increase (10x-Rx)	50	140

Timber harvesting

Timber harvest was simulated using the business-as-usual scenario developed by Maxwell et al. (2020) based on 2012 county-level timber receipts and reports from National Forests within the Klamath ecoregion. Under this scenario, most harvesting occurs on private industrial lands in the form of clear cuts and harvesting on Federal lands generally occurs with a goal of promoting old-growth characteristics through thinning operations. Harvest was parameterized to treat 278 hectares of the landscape every five years (see Appendix H).

Scenarios

To isolate the effects of prescribed fire on vegetation and fire regimes under climate change, a total of twelve scenarios were simulated using combinations of each climate and treatment scenario for a 50-year period. Each scenario was replicated three times for a total of 36 model runs (i.e., 3 climate scenarios * 4 prescribed fire scenarios * 3 replicates = 36 model runs).

Analysis

All data processing, model parameterization, model calibration, and data analyses were completed using R v4.2.0 (R Core Team, 2022) in RStudio 2022.02.03 (RStudio Team, 2022) with the following packages: dplyr (Wickham et al., 2022), ggplot2 (Wickham, 2016), ggpubr

(Kassambara, 2020), and terra (Hijman, 2022). R scripts can be found on the online repository (<https://github.com/alideak/Landis-Siskiyous-Code.git>).

Landscape-scale analyses

Aboveground carbon consumed by each ignition type was compared across scenarios. SCRPPLE calculates the mortality of aboveground biomass during each fire in g/m². The biomass consumed by each ignition type was summed across all years of the simulation, averaged across repetitions, and converted to Tg of carbon per hectare.

Burn severity was analyzed using the mean dNBR of all wildfires occurring across scenarios. To analyze the change in dNBR values through time across climate and treatment scenarios, a regression analysis was conducted using the ggpubr package (Kassambara, 2020) in R with dNBR as the dependent variable and simulation year as the independent variable. dNBR values for each year and combinations of climate and treatment scenarios were averaged across repetitions.

Burn severity was further analyzed based on the slope and aspect of cells burned during wildfire events. Slope and aspect values were derived from a 1/3 arc second digital elevation model of the landscape (US Geological Survey, 2020) and each burned cell was analyzed to find the dNBR value during wildfire events. dNBR values were averaged across repetitions of simulations based on their slope (greater than or less than 20°), aspect (north- or south-facing), and climate region for the first and last 25 years of simulations of each climate and treatment scenario.

The distributions of area burned by wildfire were analyzed to understand how climate and prescribed fire frequency and extent effected the average area burned by wildfire. Both human-accidental and lightning ignited fire data were filtered to find the largest 50% of fires in all treatment and climate scenarios across repetitions and log-transformed to achieve a normal distribution prior to conducting analysis. To compare means across scenarios, we ran Bartlett's test for homoscedasticity, followed by a one-way analysis of variance (ANOVA) using a the unique

combinations of climate and treatment scenarios as the independent variable. We also used a two-way ANOVA to with treatment and climate scenarios as the independent variables. To analyze the statistical difference between scenarios, we used post-hoc Tukey's honestly significant difference test.

Local-scale analyses

The effect of increasing prescribed fire frequency on aboveground and soil organic carbon storage was analyzed by comparing cells with prescribed fire applied at increasing frequencies and cells that had experienced a high-severity wildfire. We began by finding the amount of aboveground and soil organic carbon of every cell at each time step and the ignition type and severity of burned cells. We then summed the number of prescribed fires and wildfires that had occurred within each cell on the landscape during each simulation. To identify cells for analysis, we filtered cells to retain only cells where no wildfire occurred with between one and seven prescribed fires applied throughout the simulation at specified and equal intervals and cells that had experienced a single high-severity wildfire during the first five years of the simulation. Cells were grouped based on the type and amount of fire that occurred on each cell and climate scenario. For analysis, we calculated the mean and standard deviation of aboveground and soil organic carbon storage across these groups at one-year intervals.

Similarly, cells were isolated across all climate and treatment scenarios to understand how prescribed fire effected burn severity locally. We found all cells where wildfire was not preceded by prescribed fire and cells treated with prescribed fire and subsequently burned in wildfire events. Cells were analyzed based on the length of time between prescribed fire and wildfire events and proportion of cells burning within each severity class.

CHAPTER III.

RESULTS

Landscape-scale

The amount of aboveground carbon consumed by wildfires was lowest in the 10x-Rx scenario in all climate scenarios (Figure 3). However, the greatest total aboveground carbon consumption occurred during the 10x-Rx scenario due to carbon loss during prescribed fire events. Across climate scenarios, the largest amount of carbon consumed during wildfire events occurred in the warmer and drier climate scenario. Aboveground carbon consumed in the 10x-Rx scenario consistently remained below 100 Tg throughout the simulation period when calculated with wildfires alone but surpassed 150 Tg with carbon consumption during prescribed fire events included in the sum.

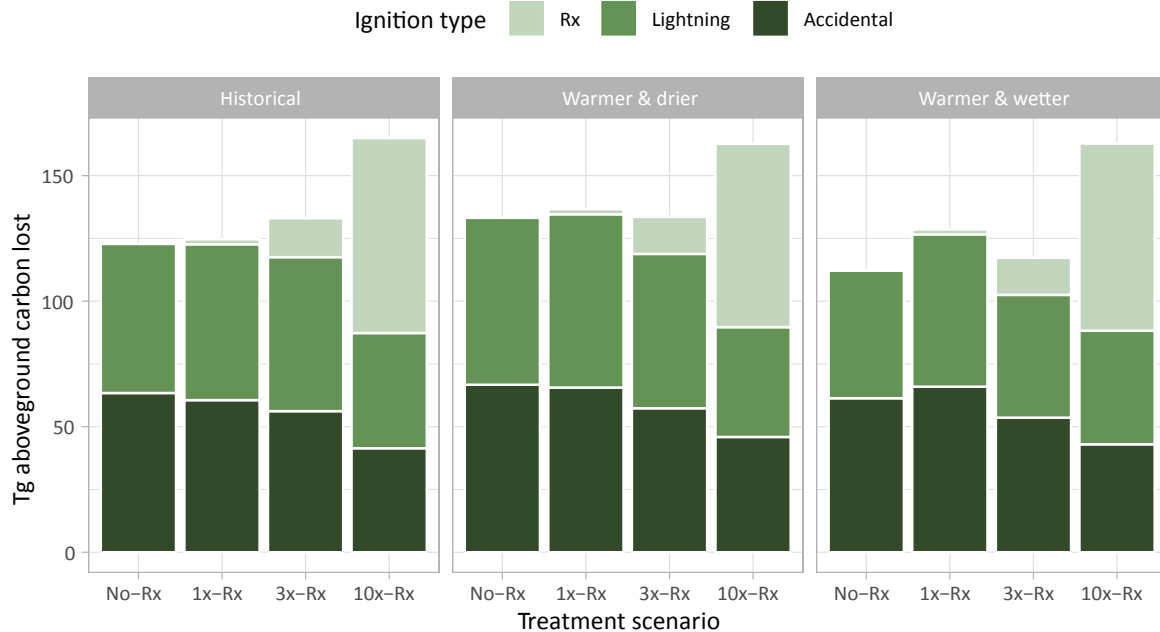


Figure 3. Average aboveground carbon consumed by ignition type during the 50-year simulations across climate and treatment scenarios. The aboveground carbon values reported are the sum of all aboveground carbon consumed during each ignition type of each simulation averaged across three repetitions of each climate and treatment scenario.

Prescribed fire produced the strongest effect in the warmer and wetter climate scenario, with mean dNBR showing a downward trend through time in every treatment scenario and the largest effect taking place in the 3x-Rx and 10x-Rx scenarios (Figure 4). Fire severity also declined across treatment scenarios in the warmer and drier climate scenario, with the greatest decrease in the no-Rx scenario. During the historical climate scenario, fire severity increased in the no-Rx and 10x-Rx scenarios but decreased in the 1x-Rx and 3x-Rx scenarios. The average fire severity on the landscape during most years was moderate and there were only one to three years during each 50-year simulation where the mean dNBR fell within the high-severity category.

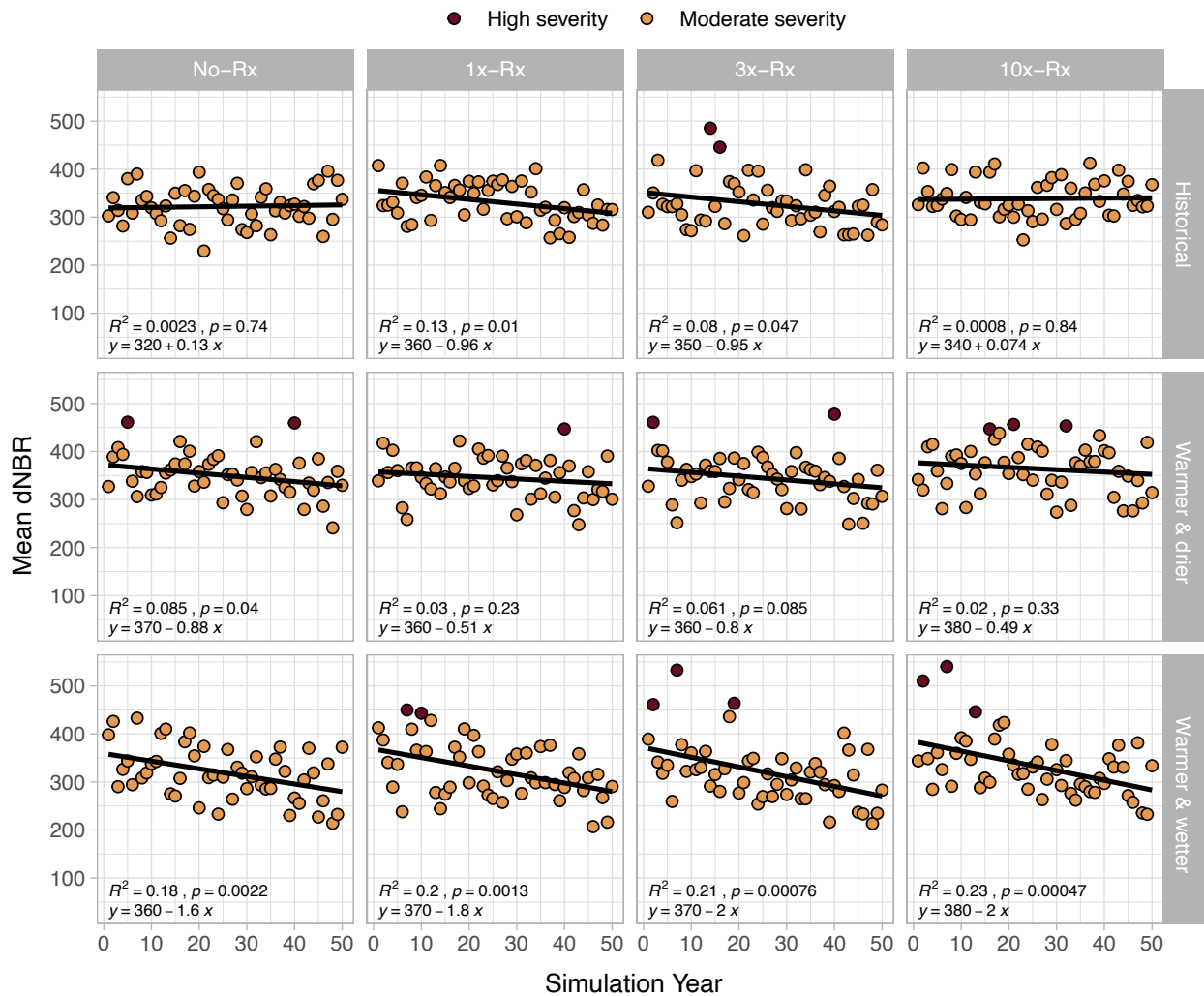


Figure 4. Change in mean burn severity, as measured by dNBR, of wildfires for each simulation year across treatment and climate scenarios

Wildfire severity was more variable when analyzed across topographic variables, climate regions, and climate scenarios (Figure 6). In a historical climate scenario, there were little to no changes in severity during the no-Rx and 10x-Rx scenarios although increases in severity occurred on in the wettest climate region (climate region 3) on south aspects in the No-Rx treatment scenario. Severity decreased across all topographies and climactic gradients in the 3x-Rx scenarios, with the greatest decreases in the third (wettest) climate region on north-facing aspects and on slopes less than 20 degrees. In a warmer and drier climate, severity decreased across all climactic and topographical variables in the third climate region, with the least change on south-facing aspects. On south-facing aspects, severity increased in the second and third climate region, with the exception that severity remained nearly the same in the driest (first) climate region in the 10x-Rx scenario. In a warmer and wetter climate scenario, severity also decreased across climactic and topographical variables although slightly increased on north-facing aspects in the 1x-Rx scenario.

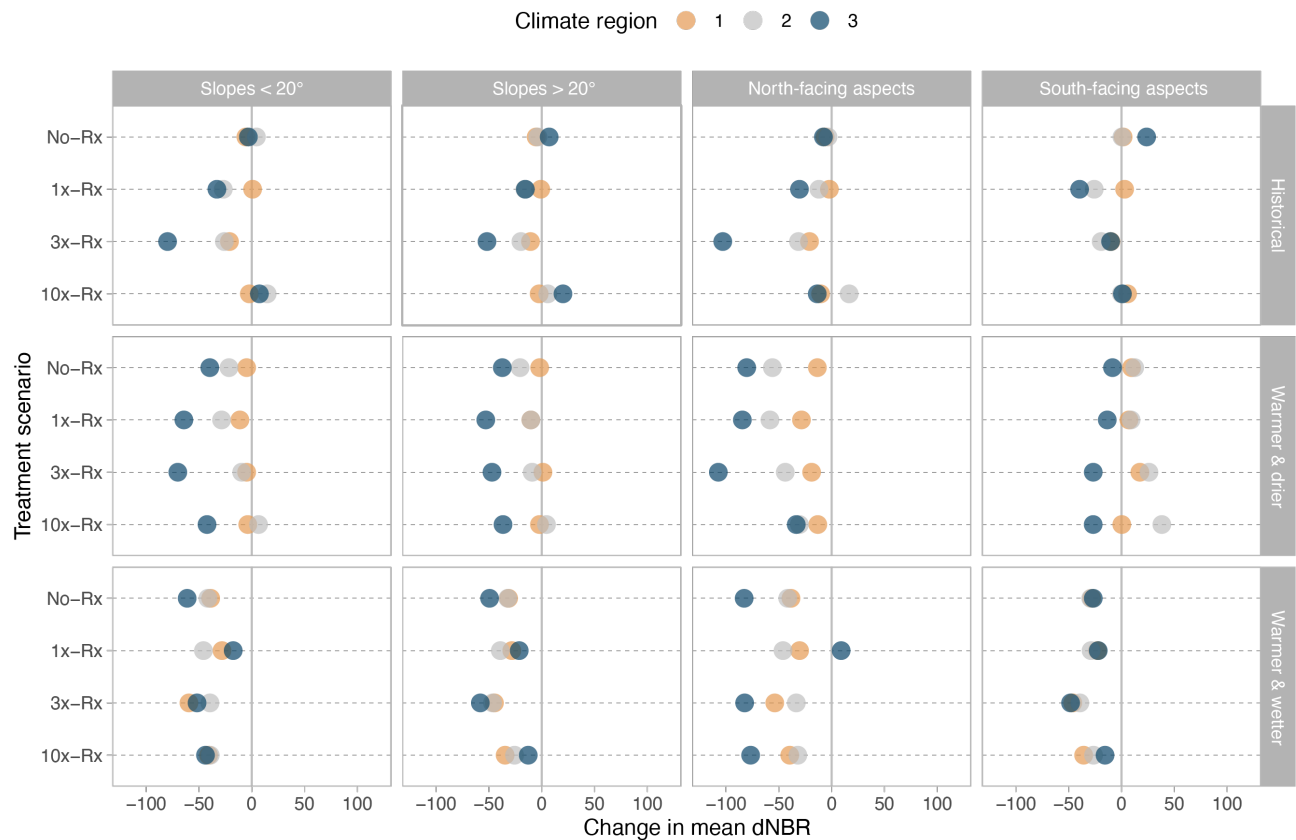


Figure 6. Change in the mean burn severity between the first and last 25 years of the simulation by treatment scenario and faceted by climate scenario and topographical variables. The color represents each of the three distinct climate regions.

The distribution of the largest 50 percent of wildfires did not vary significantly across each unique scenario (Figure 5). Upon a two-way ANOVA with treatment scenarios and climate scenarios as independent variables, significant differences were found between treatment scenarios ($p < 0.05$) and climate scenarios ($p < 0.001$). Further analysis with the Tukey’s honestly significant difference post-hoc test showed significant differences between the No-Rx and 1x-Rx scenarios and the warmer and drier climate scenario with both the historical and warmer and wetter climate scenarios ($p < 0.001$).

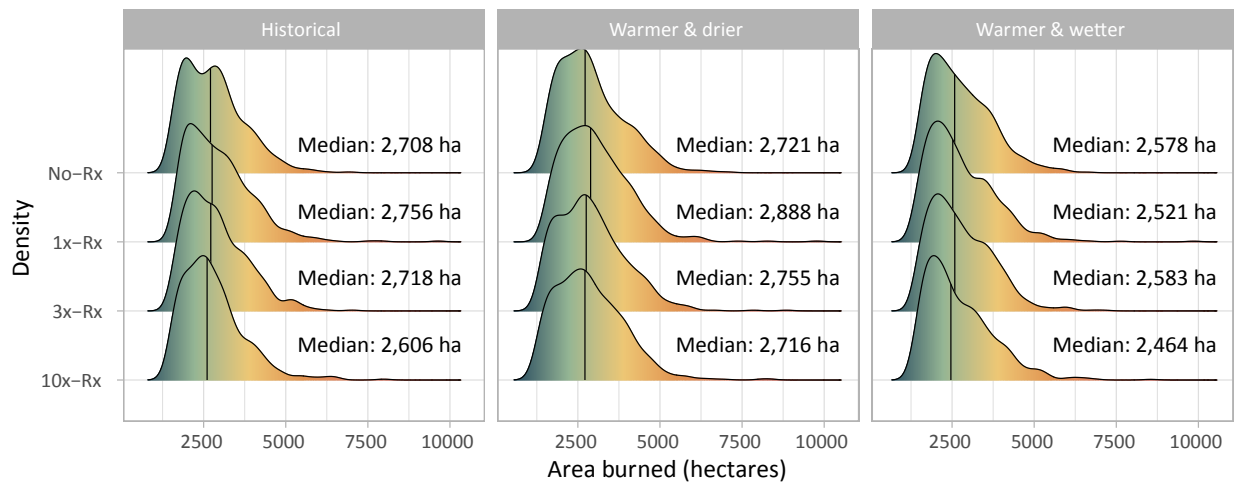


Figure 5. The distributions of area burned by the largest 25 percent of wildfires across treatment and climate scenarios. The median area burned is shown by vertical lines.

Local scale

The amount of total aboveground and soil organic carbon storage on 30-meter cells declined with increasing prescribed fire frequency with greater than three prescribed fires per 50-year period

(Figure 7). Results show that above and below ground carbon storage was maintained through time on sites where three prescribed fire treatments were ignited during a 50-year simulation period. Across climate scenarios, in cells where two prescribed fires were ignited, total carbon increased to nearly 15,000 g/m². At frequencies greater than four prescribed fires per 50-year simulation period, carbon storage declined.

In cells that experienced a high-severity fire during the first five years of the simulation, carbon storage decreased substantially below 5,000 g/m². In these cells, carbon storage showed a sharp drop in carbon storage below 5,000 g/m² that took between twenty and thirty years to rebound to the previous carbon storage amounts. In comparison, a single prescribed fire led to a slight decrease in carbon storage that quickly rebounded. These trends are consistent across climate scenarios.

When aboveground and soil organic carbon were separately analyzed, aboveground carbon decreased over the simulation period with greater than one prescribed fire per 50-year simulation period, but soil organic carbon increased until prescribed fire frequency surpassed once per ten-year simulation period and following high-severity wildfire. At a frequency of three prescribed fires per 50-years, the amount of aboveground and soil organic carbon within cells was nearly equivalent, each equaling ~5,000 g/m².

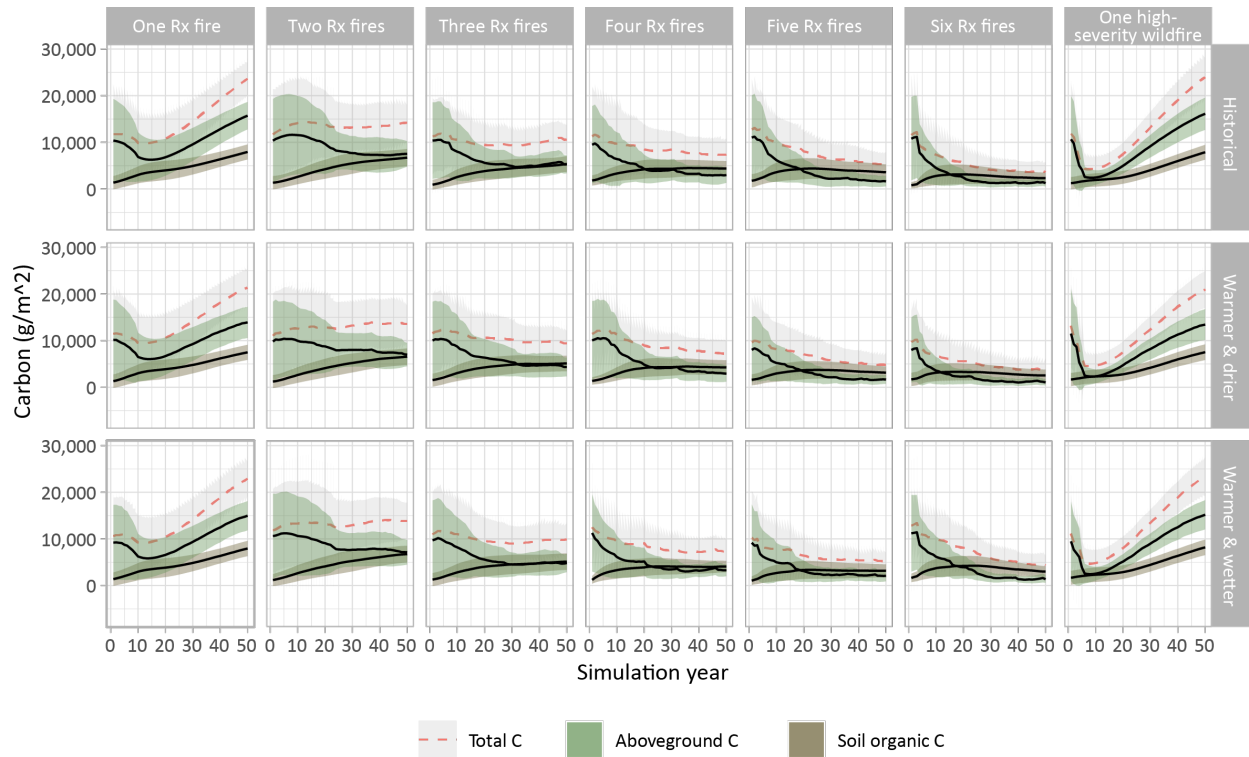


Figure 7. Mean total, aboveground, and soil organic carbon storage of cells with increasing prescribed fire treatment frequency across climate scenarios. Plots are faceted vertically by climate scenarios and horizontally by prescribed fire frequency. The error bar represents the standard deviation of each carbon pool on the landscape at each time steps.

Prescribed fire increased the likelihood of low-severity wildfires on cells following prescribed fires across climate scenarios (Figure 8). Across all climate scenarios, 11% more sites burned at a low severity during wildfires ignited in the 25 years following treatment. Cells were more likely to burn at a low severity in a warmer and wetter scenario than in the historical and warmer and drier climate scenarios.

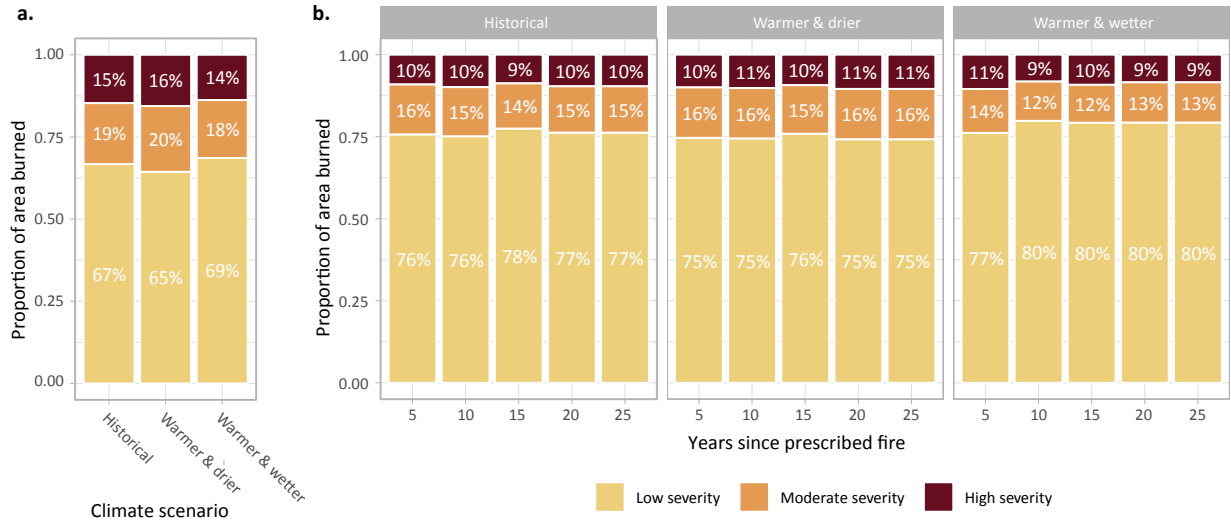


Figure 8. (a) the proportion of cells experiencing each severity class during wildfire events not preceded by wildfire events or prescribed fire across treatment and climate scenarios. (b) the proportion of cells burning at each severity class during wildfires following prescribed fire treatments. Results are shown by the number of years since the previous prescribed fire treatment and faceted by climate scenario.

CHAPTER IV.

DISCUSSION

Our hypotheses predicted that increased prescribed fire frequency would lower but stabilize above and belowground carbon storage due to lowered carbon consumption during wildfire events and decrease the severity and size of future wildfires.

Analysis at the local scale showed prescribed fire stabilized carbon storage on cells where prescribed fires was applied up to three times per 50-year simulation period. At greater prescribed fire frequencies, carbon storage declined over the simulation period. When aboveground and soil organic carbon pools were separately analyzed in cells with increasing prescribed fire frequency, we found an upward trend in soil organic carbon until prescribed fire frequency surpassed once per ten-year simulation period (similar to analysis by Pellegrini et al. (2018) finding an increase in soil organic carbon following frequent burning across conifer forest ecosystems). These results indicate a prescribed fire frequency of 15 years is adequate to maintain carbon storage at 10,000 g/m² under both drier and wetter climate change scenarios. However, attempting to increase carbon storage by using lower frequencies of prescribed fire treatments may in turn, lead to a greater potential for a high-severity fire that could ultimately destabilize long-term carbon storage (as shown by Figure 1).

As hypothesized, we found that increasing the application of prescribed fire by three and ten times the contemporary prescribed fire frequency and extent reduced aboveground carbon consumption during wildfires. Reducing aboveground carbon consumption during wildfire events has direct effects on the amount of carbon emissions emitted during wildfire events (Restaino & Peterson, 2013). As greater attention is paid to public health issues stemming from increased wildfire smoke exposure to communities, prescribed fire provides an opportunity to distribute emissions resulting from large smoke events during the wildfire season throughout the year when smoke may

be more manageable due to better burning conditions (D'Evelyn et al., 2022).

Although prescribed fire was found to lower the severity of future wildfires, it was found to be relatively ineffective at decreasing the size of wildfires. Moreover, the effects of treatment on severity and area burned at a landscape-scale was largely overshadowed by the effects of climate. On a landscape scale, we found prescribed fire produced the strongest effects in the warmer and wettest climate scenario and within the wettest climate region on the landscape. In a warmer and drier climate scenario, there were minimal changes in the driest climate region, increases in severity on south-facing aspects, and the largest area burned during wildfire events occurred. At a local scale, prescribed fire was effective at lowering the severity of future wildfires, especially in the warmer and wetter climate change scenario.

Combined, these findings suggest that the placement of treatments matters. Targeting treatments in areas of social-ecological concern, such as near the wildland-urban interface and areas with high ecological or cultural value, and within climactic gradients and topographies found to be most effective for reducing fire severity will provide opportunities for managers to decrease the risk of high-severity wildfire. Targeting treatments further allows land managers to leverage existing treatments and take advantage of limited funding and capacity for fuels reduction projects to reduce fire risk at scale (North et al., 2021). Forest managers may also want to consider alternative management solutions under divergent climate change scenarios when considering the placement of treatments.

Limitations

Fuels reduction techniques, such as thinning, were not intentionally placed to precede prescribed fire on the landscape. These treatments have been found to be important for influencing the behavior of prescribed fires and the spread of wildfires on the landscape. This may have

contributed to the elevated losses of carbon from prescribed fire and increased prescribed fire frequency and extent not having the expected effects on wildfire severity and area burned at a landscape-scale.

It is also important to recognize that the study area exists within a larger landscape and was parameterized to only show the impacts of fires ignited within its borders. Although outside the scope of this study, forest management, climate change, and disturbance on the surrounding landscape also plays an important role in determining the trajectory of fire regimes and vegetation within the study area and across the larger landscape.

CHAPTER V.

CONCLUSION

The 2022 Wildfire Crisis Strategy (USFS, 2022) recognized the east slope of the Siskiyou Mountains as one of 29 landscapes at high-risk for catastrophic wildfires with shovel-ready projects in the US although it was not awarded initial investments for fuels reduction projects through the Bipartisan Infrastructure Law. As more funding sources become available for this work, it is important to consider how treatments may impact the landscape, the appropriate frequency and extent of prescribed fire needed to restore fire-adapted ecosystems, and how differing climate scenarios may affect how prescribed fire impacts the landscape.

As climate change mitigation strategies increasingly turn towards natural climate solutions, forest management has received much attention for its ability to mitigate the global impacts of climate change through carbon sequestration (Griscom et al., 2017; Silva et al., 2022). Although prescribed fire could be viewed as a threat to carbon storage and fire suppression has increased carbon storage in forests over the past century, this carbon is increasingly vulnerable to combustion during high-severity wildfire events. Properly used at the correct frequency, prescribed fire has the potential to maintain carbon storage while having tangible effects on other land management goals, including biodiversity conservation, scenic and recreational value of landscapes, and reduced fire risk to adjacent communities.

Our study showed a prescribed fire frequency of 15 years suitable for stabilizing aboveground and soil organic carbon storage in all climate scenarios. With increased funding, Federal agencies may have increased capacity to implement treatments to reduce fire risk. Our results suggest that by treating priority locations on public lands with the highest potential for catastrophic wildfires and at this prescribed fire frequency, managers can proactively reduce the

likelihood that these areas will experience destabilizing effects on carbon storage, reduce the amount of carbon lost during wildfire events, and reduce the severity of wildfires locally. Coupling thinning treatments with prescribed fire may further improve the outcomes of these management actions.

We suggest future research explore how similar treatments may alter results over longer time periods with treatments more strategically placed across the landscape. More treatments may be located to leverage existing treatments and burned areas, as well as to protect wildland-urban interface communities. Future research may also quantify the funding and workforce capacity required to implement such treatments to inform realistic management solutions.

APPENDICES

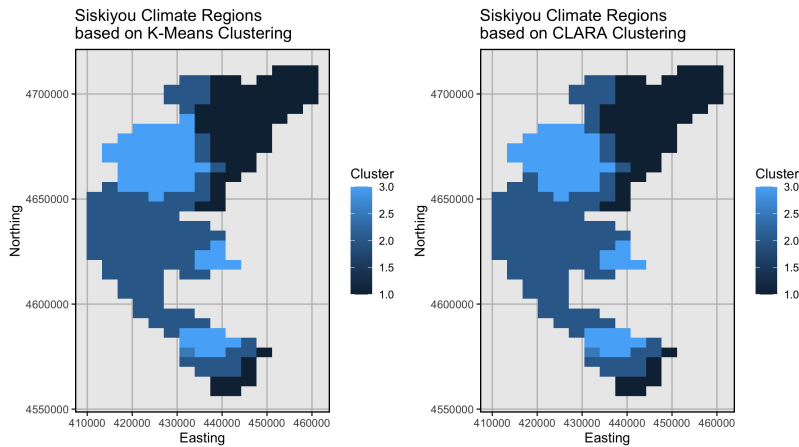
APPENDIX A. CLIMATE REGION CLASSIFICATION

1.

Cropped 30-year average (1991-2020) precipitation, maximum temperature, and minimum temperature values for months during the growing season (i.e., months with an average temperature greater than 5°C) at 4-km resolution from the PRISM Climate Group (2021) to the study landscape.

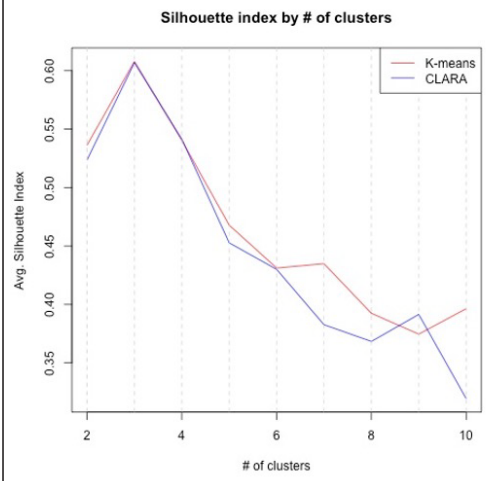
2.

Determined which areas of the landscape had homogenous climates using unsupervised classification through two methods: K-Means clustering and CLustering LARge Applications (CLARA).



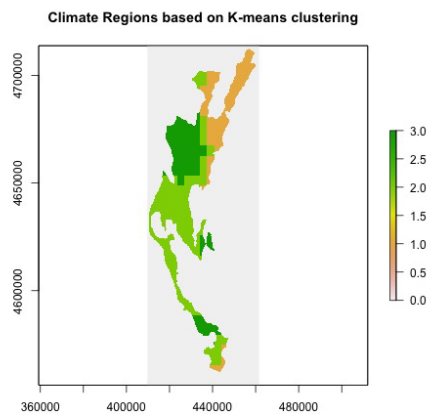
3.

Silhouette index used to evaluate the performance of the unsupervised classification methods, whereas higher silhouette indices indicate higher performance (on a scale of -1 to 1). K-means clustering was found to have a slightly higher silhouette index.



4.

Reprojected and masked raster produced by K-Means clustering analysis to match the resolution and spatial extent of the study landscape.

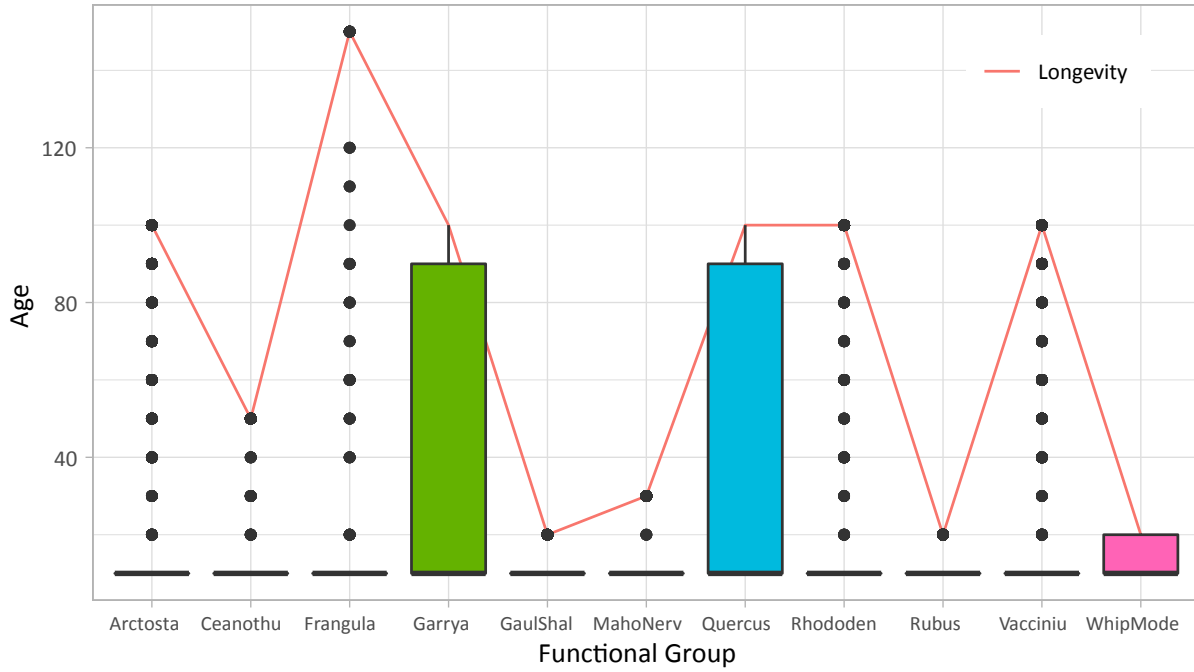


APPENDIX B. SPECIES SIMULATED

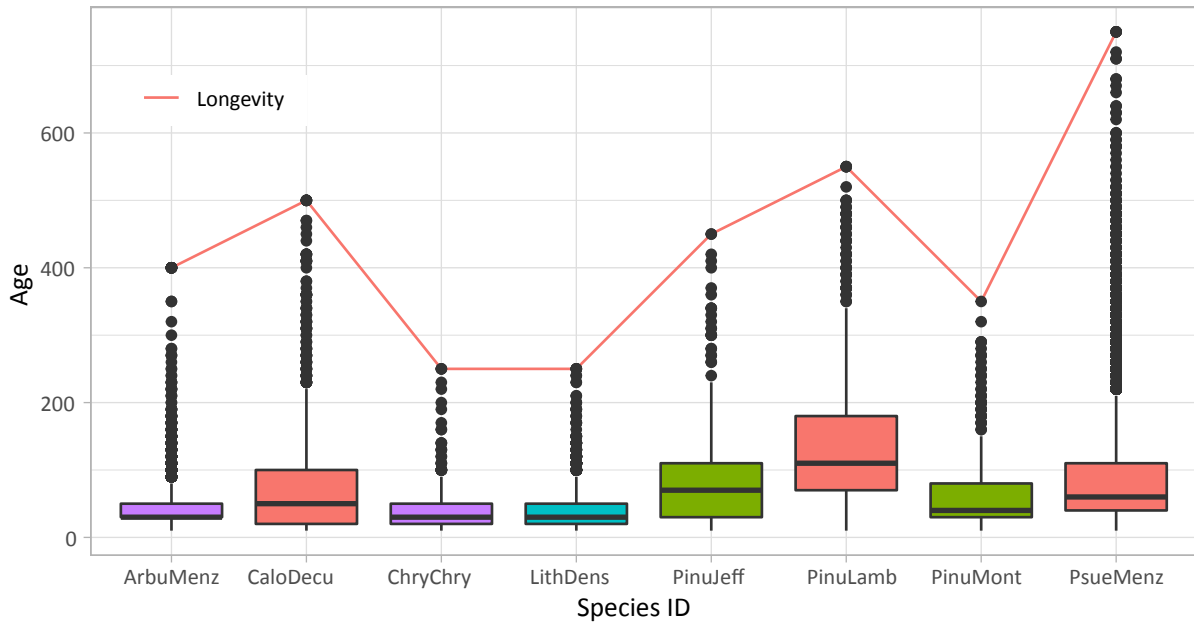
Species ID	Scientific name	Common name	Functionalgroup
ArbuMenz	<i>Arbutus menziesii</i>	Pacific madrone	Hardwood
Arctosta	<i>Arctostaphylos canascens</i>	Hoary manzanita	Shrub_xeric
Arctosta	<i>Arctostaphylos columbiana</i>	Hairy manzanita	Shrub_xeric
Arctosta	<i>Arctostaphylos nevadensis</i>	Pinemat manzanita	Shrub_xeric
Arctosta	<i>Arctostaphylos patula</i>	Greenleaf manzanita	Shrub_xeric
Arctosta	<i>Arctostaphylos viscida</i>	Whiteleaf manzanita	Shrub_xeric
CaloDecu	<i>Calocedrus decurrens</i>	California incense cedar	Conifer
Ceanothu	<i>Ceanothus cuneatus</i>	Buck brush	Shrub_xeric
Ceanothu	<i>Ceanothus pumilus</i>	Dwarf ceanothus	Shrub_xeric
Ceanothu	<i>Ceanothus velutinus</i>	Snowbrush ceanothus	Shrub_xeric
ChryChry	<i>Chrysolepis chrysophylla</i>	Golden chinquapin	Hardwood
Frangula	<i>Frangula californica</i>	Coffeeberry	Shrub_xeric
Frangula	<i>Frangula purshiana</i>	Cascara	Shrub_xeric
Garrya	<i>Garrya buxifolia</i>	Boxleaf silk tassel	Shrub_xeric
Garrya	<i>Garrya fremontii</i>	Bearbrush	Shrub_xeric
GaulShal	<i>Gaultheria shallon</i>	Salal	Shrub_mesic
MahoNerv	<i>Mabonia nervosa</i>	Cascade barberry	Shrub_mesic
NothDens	<i>Lithocarpus densiflora</i>	Tanoak	Hardwood
PinuJeff	<i>Pinus jeffreyi</i>	Jeffrey pine	Conifer
PinuLamb	<i>Pinus lambertiana</i>	Sugar pine	Conifer
PinuMont	<i>Pinus monticola</i>	Western white pine	Conifer
PseuMenz	<i>Pseudotsuga menziesii</i>	Douglas fir	Conifer
Quercus	<i>Quercus sadleriana</i>	Deer oak	Shrub_xeric
Quercus	<i>Quercus vaccinifolia</i>	Huckleberry oak	Shrub_xeric
Rhododen	<i>Rhododendron macrophyllum</i>	Pacific rhododendron	Shrub_mesic
Rhododen	<i>Rhododendron occidentale</i>	Western azalea	Shrub_mesic
Rubus	<i>Rubus leucodermis</i>	Whitebark raspberry	Shrub_mesic
Rubus	<i>Rubus parviflorus</i>	Thimbleberry	Shrub_mesic
Rubus	<i>Rubus ursinus</i>	Pacific blackberry	Shrub_mesic
Vacciniu	<i>Vaccinium ovatum</i>	Evergreen huckleberry	Shrub_mesic
Vacciniu	<i>Vaccinium parvifolium</i>	Red huckleberry	Shrub_mesic
WhipMode	<i>Whipplea modesta</i>	Common whipplea	Shrub_mesic

APPENDIX C. TREE AND SHRUB AGES

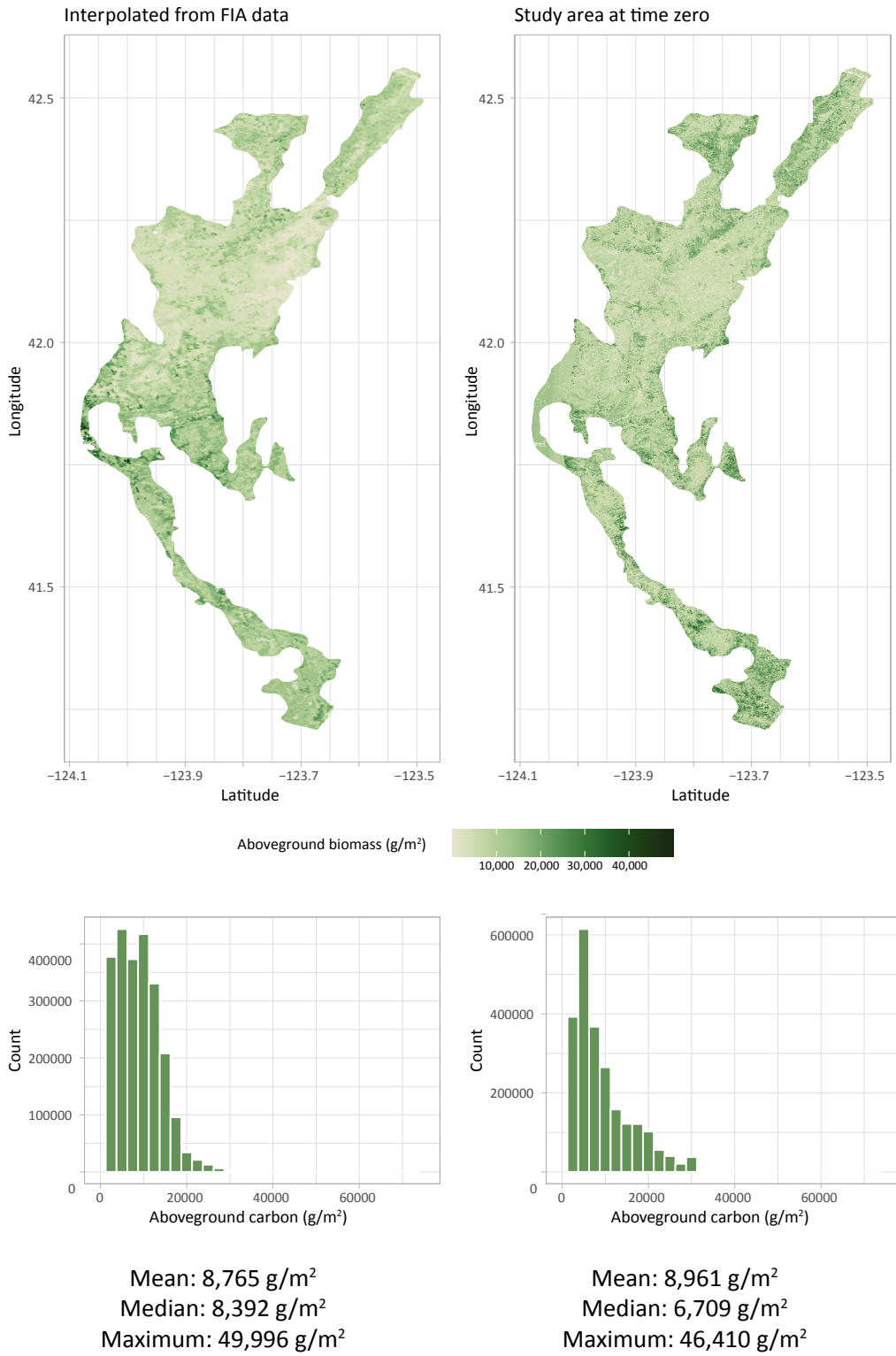
Shrub Functional Group Ages



Tree Ages based on Inland California and Southern Cascades FSV Site Index Equations



APPENDIX D. ABOVEGROUND CARBON STORAGE



APPENDIX E. NECN SPECIES PARAMETERIZATION TABLE

Species	N Fixer	GDD Min*	GDD Max*	Min January Temp (c)	Drought Tolerance	Leaf Longevity	Epicormic Resprout	Lignin Content			
								Leaf	Fine Root	Wood	Coarse Root
ArbuMenz											
CaloDecu											
ChryChry											
NothDens											
PinuJeff					10						
PinuLamb											
PinuMont											
PseuMenz											
Arctosta		2	2	2	10			18	32	14	31
Ceanothu		3	3	3	9			16		16	
Frangula		8	8	8	9			15		15	
Garrya					12	30					
GaulShal		6	6	6	9	30		32	32		
MahoNerv		7	7	7	9	30					
Quercus		1	1	1	1	1	1	1	1	1	1
Rhododen					9			32	32		
Rubus		5	5	5	9			25		20	
Vacciniu					9			26	11	17	
WhipMode		6	6	6	12						

SOURCES	
Estimated based on known parameters of other species	FRED database (Iversen et al., 2021)
Thompson et al. (2015)	Neill & Puettmann (2013)
Thompson et al. (2006)	Copeland & Harrison (2015)
Estimation based on Thompson et al. (2006) & Thompson et al. (2015)	Huff et al. (2018)
Serra-Diaz et al. (2018)	National Ecological Observatory Network (2021)
TRY database (Kattge et al., 2020)	Meerdink et al. (2016)
Loudermilk et al. (2014)	Friesen (1991)
Berner & Law (2016)	Rundel (1979)
Fire Effects Information System (Abrahamson, n.d.)	Paramaterized using HydroPSO

Species	C:N Ratio					Max ANPP	Max Biomass
	Leaf	Fine Root	Wood	Coarse Root	Litter		
ArbuMenz							
CaloDecu							
ChryChry							
NothDens							
PinuJeff							
PinuLamb							
PinuMont							
PseuMenz							
Arctosta		32					
Ceanothu		11					
Frangula							
Garrya							
GaulShal		32					
MahoNerv							
Quercus	1	1	1	1	1		1
Rhododen	13	11					
Rubus		11			22		
Vacciniu		11			22		
WhipMode							

Footnotes

- ¹ Based on *Quercus chrysolepsis* - According to Nixon (2002) *Quercus vaccinifolia* falls into the oak subgroup golden oaks, and *Quercus chrysolepsis* was the only golden oak species available in the database.
- ² Based on *Arctostaphylos pringlei*, the only manzanita in the database
- ³ GDD based on the min and max of and temp based on mean of *Ceanothus spinosus* and *Ceanothus thyrsiflorus*, the only two Ceanothus species in the database
- ⁴ Based on mean between *Vaccinium parvifolium* and *Vaccinium ovalifolium*
- ⁵ Based on *Rubus parviflorus*; GDD Max based on *Whipplea modesta* - couldn't get cohorts to reproduce with such a low GDD max
- ⁶ Given a min january temp of -1 and GDD matching *Arbutus menziesii* because according to https://www.dnr.wa.gov/publications/amp_nh_whimod.pdf Whipplea modesta is often found alongside *Gaultheria shallon* (GaulShal) and *Arbutus menziesii* (ArbuMenz); GaulShal distribution closely matches *Arbutus menziesii* as well so also GDD and min temp also assigned same GDD and min temp as ArbuMenz
- ⁷ Based on *Berberis fremontii*
- ⁸ Based on min and max of *Frangula californica* and *Frangula purshiana*

- ⁹ For those associated with the TRY database, if the species tolerance to drought was designated as low, medium or high, it was given a drought tolerance of 0.7, 0.8, or 0.9, respectively. If it was given an integer value of 1-5 (with 1 being low tolerance to drought), it was given a drought tolerance of 0.7 (if 1 or 2, rounded), 0.8 (3 or 4, rounded), or 0.9 (5, rounded).
If multiple species within a functional group had different drought tolerances, the value was averaged (for example, *Ceanothus cuneatus* has a high drought tolerance and *Ceanothus velutinus* has a low drought tolerance, so the *Ceanothus* functional group was given a drought tolerance of 0.8).
- ¹⁰ If described as "drought tolerant," they were given a tolerance of 0.9
- ¹¹ Based on mean fine root C:N ratio for all within genus in database - shifted up to 40 because cohorts wouldn't reproduce otherwise
- ¹² Described as being drought tolerant, so given a tolerance of 0.9
- ¹³ Based on mean of *Rhododendron macrophyllum* and *R. occidentale*
- ¹⁴ Based on *Arctostaphylos viscida*
- ¹⁵ Based on *Frangula californica*
- ¹⁶ Based on *Ceanothus cuneatus*
- ¹⁷ Based on *Vaccinium parvifolium*
- ¹⁸ Based on *Arctostaphylos glandulosa*
- ¹⁹ Based on mean of *Quercus agrifolia*, *Q. douglasii*, and *Q. lobata*
- ²⁰ Based on *Rubus ursinus*
- ²¹ Based on *Arctostaphylos uva-ursi*
- ²² Based on the mean of all species with genus in database, from Quedsted et al, 2003
- ²³ Based on *Rubus allegheniensis*
- ²⁴ Based on mean of *Rubus phoenicolasius* and *R. saxatilis*
- ²⁵ Based on *Rubus saxatilis*
- ²⁶ Based on mean of *Vaccinium myrtillus*, *V. uliginosum*, and *V. vitis-idaea*
- ²⁷ Based on root C:N ratio for *Ceanothus fendleri*
- ²⁸ Based on mean fine root C:N for *Frangula alnus* and *F. caroliniana* - the only *Frangula* species in FRED database
- ³⁰ FEIS describes these species as evergreen, similar to *Arctostaphylos*, therefore, leaf longevity was set at 1.5 years to mirror the leaf longevity of *Arctostaphylos*
- ³¹ According to Kron et al., *Arctostaphylos* spp. is phylogenetically closely related to *Arbutus Menziesii* so unknown parameters were set to match those of *A. menziesii*
- ³² Based on mean of *Ericaceae* spp in TRY database
- * GDD Min based on 1% and GDD Max based on 99% GDD on 5° base in Thompson et al. (2006) and Thompson et al., 2005

APPENDIX F. VALIDATION OF LANDIS-II INITIAL COMMUNITIES MAP USING LAI FROM REMOTE SENSING PRODUCTS

Methods

As LANDIS-II computes and produces LAI maps for June of each timestep, it is possible to validate the initial communities map interpolated for the study area using remotely sensed data. Although there are several of these products available, I chose the following two remote sensing products to do so: (1) MOD15A2H Moderate Resolution Imaging Spectroradiometer (MODIS) Level 4, Combined Fraction of Photosynthetically Active Radiation (FPAR) and LAI product (Myneni & Park, 2015) and (2) Ice, Cloud, and Land Elevation Satellite-2 (ICESat-2) ATL03 product (Neumann et al., 2021). MODIS offers four Level 4, Combined FPAR and LAI products: 500-meter composite datasets produced at 4- and 8-day intervals for data acquired by the Terra and Aqua satellites or solely the Terra satellite. The algorithm used to calculate LAI is based on empirical relationships between normalized differenced vegetation index values calculated from MODIS red and near-infrared bands and known LAI values for 13 known biomes and landcover types (Mu et al., 2013). These FPAR/LAI products are widely used for analyzing LAI over large land areas and have been found to perform reasonably well within a certainty of ± 1 LAI (Yan et al., 2016).

Using the MODIS/VIIRS Land Products Global Subsetting and Visualization Tool (ORNL DAAC, 2018), MOD15A2H Version 6 MODIS Level 4, Combined FPAR/LAI 4-day composite data acquired by the Terra satellite was acquired for the study landscape for the time period between June 1 and June 4, 2020. These data were reprojected to 30-meter resolution and masked to the extent of the initial communities map. Invalid data values were filtered, and the raster was multiplied by the recommended scale factor of 0.01 to derive estimated LAI across the landscape

NASA launched ICESat-2 in September 2018 carrying the Advanced Topographic Laser Altimeter System (ATLAS), an instrument that actively maps surface elevation using a 532-nm laser and photon-counting detection technology. The laser is split into six beams arranged in pairs of two (a strong and weak beam) spaced approximately 3.3-km apart (A. L. Neuenschwander & Magruder, 2019). Through this

technology, the ATL03 product is acquired; this product provides the height above the WGS84 ellipsoid (i.e., elevation), latitude, longitude, and time of all photon data recaptured by the ATLAS instrument which has recently been used for the first to time by Zhang et al. (2021) to effectively estimate LAI. ICESat-2 ATL03 data (Neumann et al., 2021) acquired on June 2, 2020, between latitudes of 41 and 43° north and longitudes of 123 and 124° west were downloaded. Using the Photon Research and 4 Engineering Analysis Library v3.28 (PhoREAL) toolbox, the number of photons returning from the ground and canopy and descriptive statistics for ground and canopy elevation were computed from beams one, three, and five for all photons returned from 0.01° latitude segments along each beam. Strong beams were selected for analysis because Neuenschwander et al. (2020) Neuenschwander et al. (2020) found that canopy heights were significantly underestimated by weak beams. LAI for each 0.01° latitude segment was calculated along each beam's track using Zhang et al.'s (2021) equation:

$$LAI = \frac{C}{G} \times \ln \left(1 + \frac{R_v}{\frac{\rho_v}{\rho_g} \times R_g} \right)$$

where C is the clumping index, G is the distribution of foliage, ρ_v is the number of photons returned from the canopy (v), R_g is the number of photons returned the ground (g), and $\frac{\rho_v}{\rho_g}$ is the ratio of canopy and ground reflectance. A clumping index of 0.69 was used based on a mean clumping index for mixed leaf tree cover (Chen et al., 2005). Assuming distribution of canopy foliage is random on the landscape, G equaling 0.5 was input, similar to Zhang et al (2021) and $\frac{\rho_v}{\rho_g}$ was input as 1/3 following methods used by Neuenschwander and Magruder (2016). Using the minimum and maximum latitude and longitude values provided in the statistics calculated with PhoREAL, it was possible to find all LANDIS-II and MODIS cells within the same spatial extent and calculate descriptive statistics that could then be compared to the ICESat-2 LAI values. To avoid allowing outliers to have undue influence on LAI, median values for both LANDIS-II and MODIS cells within each 0.1° ICESat-2 segment were calculated and analyzed.

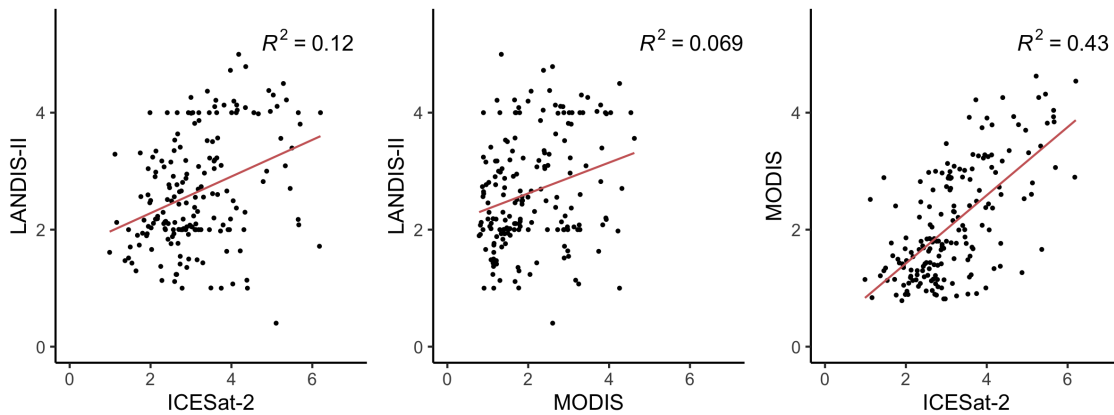
Results

Overall, LANDIS-II LAI values fell within the range of values as expected by ICESat-2 and MODIS.

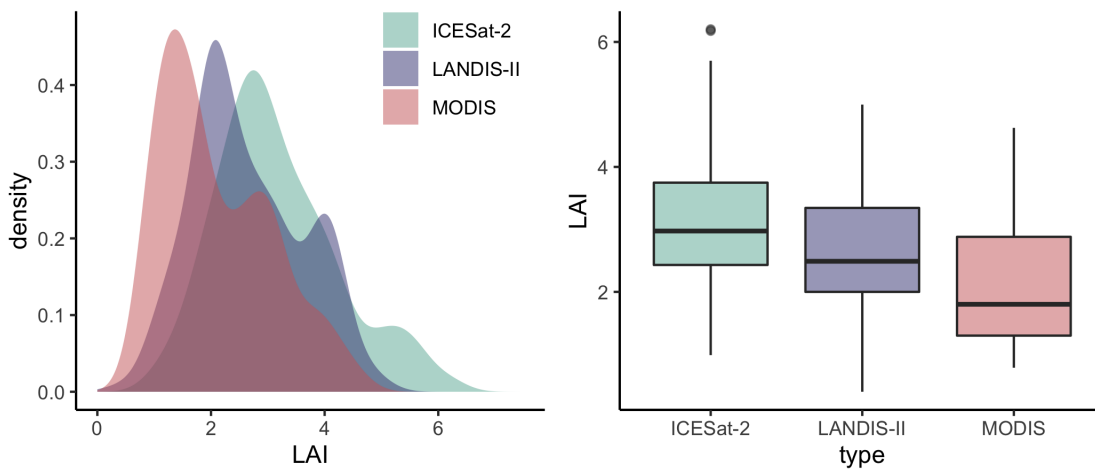
ICESat-2 was found to have a marginally larger mean LAI value (of 3.2) than LANDIS-II and MODIS with mean LAI values of 2.6 and 2.1, respectively. ICESat-2 also showed the largest range in LAI values, varying from a minimum LAI of 1.0 to a maximum LAI of 6.2. LANDIS-II ranged from 0.4 to 5.0 while MODIS had the smallest range of values, from 0.8 to 4.6.

Although, LANDIS-II did not show a clear relationship with either ICESat-2 or MODIS LAI values, LAI values from ICESat-2 and MODIS demonstrated agreement among one another suggesting some reliability in the estimation of LAI between both methods. ICESat-2 however did appear to produce larger values than expected by MODIS.

Comparison of LANDIS-II derived LAI values for cells in initial communities map to ICESat-2 and MODIS derived LAI values

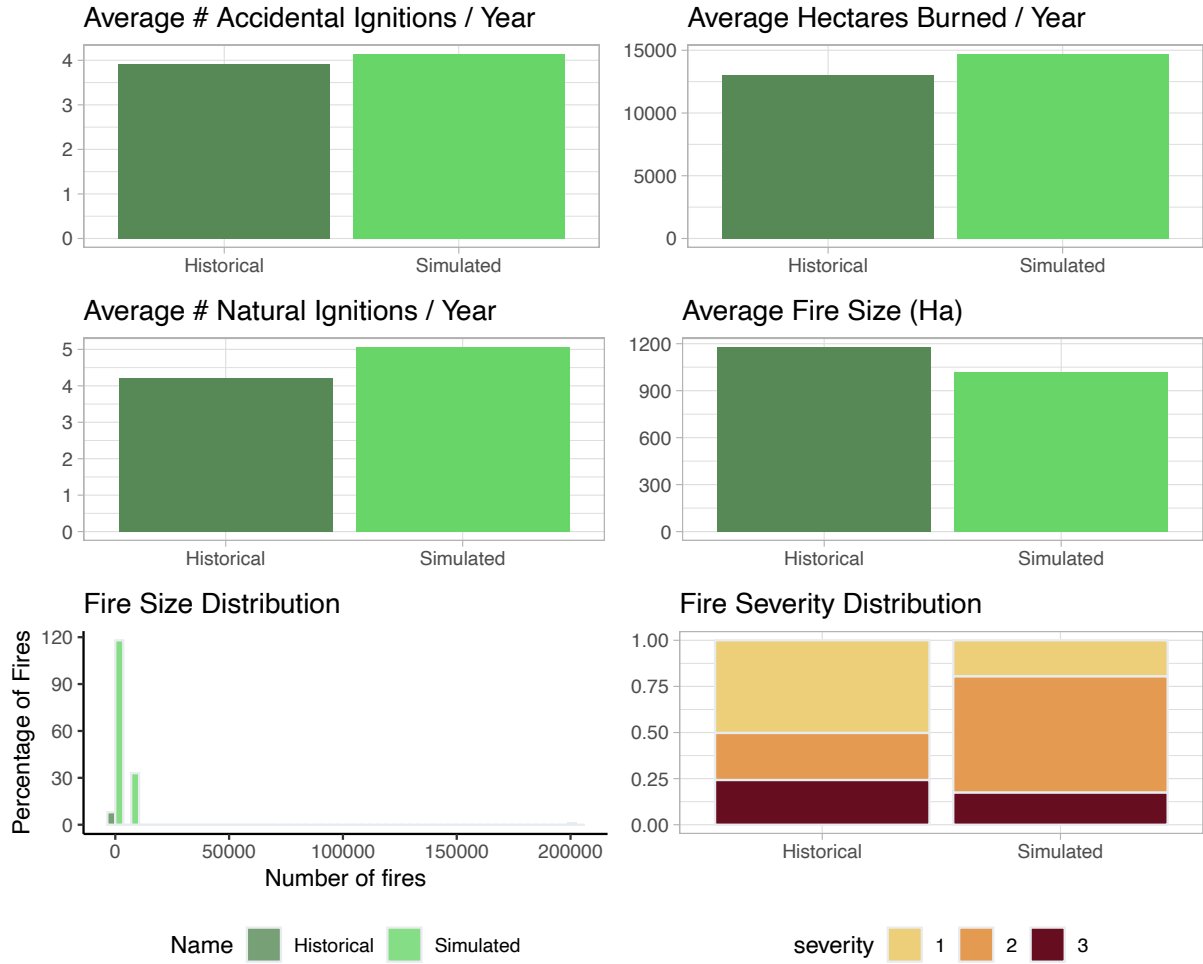


Comparison of LANDIS-II initial communities LAI values to LAI value derived from ICESat-2 and MODIS



APPENDIX G. SCRPPLE FIRE CALIBRATION

50 year simulation results compared to historic stats (1992–2018)



APPENDIX H. TIMBER HARVEST SCENARIOS

Source: Maxwell et al, 2020

Owner ship	# of cells	Hectares	Prescription	Proportion landscape	Area harvested (per 5-year timestep)
2	801,797	72,162	Large scale thinning: punching holes in canopy to promote old growth structure	9.2%	0.08%
2	801,797	72,162	Sudden oak death sanitation	9.2%	0.02%
2	801,797	72,162	Promotion of sugar pine, removal of competition	9.2%	0.02%
2	801,797	72,162	Reduce fire risk by reducing ladder fuels, (remove trees < 14 inches dbh)	9.2%	0.11%
2	801,797	72,162	Reduce fire risk by reducing ladder fuels, using mechanical thinning (remove trees < 30 inches dbh)	9.2%	0.11%
5	75,102	6,760	Timber harvest clear cut with replanting	1.0%	0.03%
5	75,102	6,760	Post disturbance replanting	1.0%	0.01%
6	40,367	3,633	Timber harvest small clear cut with replanting	1.3%	0.02%
6	40,367	3,633	Post disturbance replanting	1.3%	0.01%
7	106,894	9,620	Large scale thinning: punching holes in canopy to promote old growth structure	4.2%	0.04%
7	106,894	9,620	Sudden oak death sanitation	4.2%	0.01%
7	106,894	9,620	Promotion of sugar pine, removal of competition	4.2%	0.01%
7	106,894	9,620	Low intensity fire based on 4-ft flame length	4.2%	0.01%
7	106,894	9,620	Mixed Lethal Fire based on 6-ft flame length	4.2%	0.01%
7	106,894	9,620	Reduce fire risk by reducing ladder fuels, (remove trees < 14 inches dbh)	4.2%	0.03%
7	106,894	9,620	Reduce fire risk by reducing ladder fuels, using mechanical thinning (remove trees < 30 inches dbh)	4.2%	0.05%
7	106,894	9,620	Timber harvest patch cut with replanting	4.2%	0.02%
8	128,710	11,584	Low intensity fire based on 4-ft flame length	6.6%	0.01%
8	128,710	11,584	Mixed Lethal Fire based on 6-ft flame length	6.6%	0.01%
8	128,710	11,584	Reduce fire risk by reducing ladder fuels, (remove trees < 14 inches dbh), small target area	6.6%	0.04%
8	128,710	11,584	Reduce fire risk by reducing ladder fuels, using mechanical thinning (remove trees < 30 inches dbh)	6.6%	0.04%

Source: Maxwell et al, 2020

Ownerships

² Federal, BLM and non-specified FS lands

⁷ Wilderness area treatments

⁵ Private industrial forest lands

⁸ Wildland urban interface

⁶ Private non-industrial forest lands

REFERENCES CITED

- Abatzoglou, J. T. (2013). Development of gridded surface meteorological data for ecological applications and modelling. *International Journal of Climatology*, 33(1), 121–131. <https://doi.org/10.1002/joc.3413>
- Abatzoglou, J. T., & Brown, T. J. (2012). A comparison of statistical downscaling methods suited for wildfire applications. *International Journal of Climatology*, 32(5), 772–780. <https://doi.org/10.1002/joc.2312>
- Abatzoglou, J. T., Dobrowski, S. Z., Parks, S. A., & Hegewisch, K. C. (2018). *Terraclimate, a high-resolution global dataset of monthly climate and climatic water balance from 1958-2015*.
- Abrahamson, I. (n.d.). *Fire Effects Information System*. <https://www.feis-crs.org/feis/>
- Adlam, C., Almendariz, D., Goode, R. W., Martinez, D. J., & Middleton, B. R. (2021). Keepers of the Flame: Supporting the Revitalization of Indigenous Cultural Burning. *Society & Natural Resources*, 0(0), 1–16. <https://doi.org/10.1080/08941920.2021.2006385>
- Agee, J. (1991). Fire history along an elevational gradient in the Siskiyou Mountains, Oregon. *Northwest Science*, 65(4), 188–199.
- Agee, J. (1993). Fire Effects on Vegetation. In *Fire Ecology of Pacific Northwest Forests* (pp. 113–150). Island Press.
- Agee, J. (2005). The Complex Nature of Mixed-Severity Fire Regimes. In L. Taylor, J. Zelnik, S. Cadwallader, & B. Highes (Eds.), *Mixed severity fire regimes: Ecology and management symposium proceedings* (p. 10). Association of Fire Ecology.
- Asner, G. P., Scurlock, J. M. O., & A. Hicke, J. (2003). Global synthesis of leaf area index observations: Implications for ecological and remote sensing studies. *Global Ecology and Biogeography*, 12(3), 191–205. <https://doi.org/10.1046/j.1466-822X.2003.00026.x>
- Berner, L. T., & Law, B. E. (2016). Plant traits, productivity, biomass and soil properties from forest sites in the Pacific Northwest, 1999–2014. *Scientific Data*, 3(1), 160002. <https://doi.org/10.1038/sdata.2016.2>
- Burns, R. M., & Honkala, B. H. (1990). *Silvics of North America: 1. Conifers; 2. Hardwoods*. (Agriculture Handbook No. 654; p. 877). USDA Forest Service. https://www.srs.fs.usda.gov/pubs/misc/ag_654/table_of_contents.htm

- Cansler, C. A., Hood, S. M., Varner, J. M., van Mantgem, P. J., Agne, M. C., Andrus, R. A., Ayres, M. P., Ayres, B. D., Bakker, J. D., Battaglia, M. A., Bentz, B. J., Breece, C. R., Brown, J. K., Cluck, D. R., Coleman, T. W., Corace, R. G., Covington, W. W., Cram, D. S., Cronan, J. B., ... Wright, M. C. (2020). The Fire and Tree Mortality Database, for empirical modeling of individual tree mortality after fire. *Scientific Data*, 7(1), 194. <https://doi.org/10.1038/s41597-020-0522-7>
- Cassell, B. A., Scheller, R. M., Lucash, M. S., Hurteau, M. D., & Loudermilk, E. L. (2019). Widespread severe wildfires under climate change lead to increased forest homogeneity in dry mixed-conifer forests. *Ecosphere*, 10(11), e02934. <https://doi.org/10.1002/ecs2.2934>
- Chen, J. M., Menges, C. H., & Leblanc, S. G. (2005). Global mapping of foliage clumping index using multi-angular satellite data. *Remote Sensing of Environment*, 97(4), 447–457. <https://doi.org/10.1016/j.rse.2005.05.003>
- Cochrane, M. A., Moran, C. J., Wimberly, M. C., Baer, A. D., Finney, M. A., Beckendorf, K. L., Eidenshink, J., Zhu, Z., Cochrane, M. A., Moran, C. J., Wimberly, M. C., Baer, A. D., Finney, M. A., Beckendorf, K. L., Eidenshink, J., & Zhu, Z. (2012). Estimation of wildfire size and risk changes due to fuels treatments. *International Journal of Wildland Fire*, 21(4), 357–367. <https://doi.org/10.1071/WF11079>
- Copeland, S. M., & Harrison, S. P. (2015). Identifying plant traits associated with topographic contrasts in a rugged and diverse region (Klamath-Siskiyou Mts, OR, USA). *Ecography*, 38(6), 569–577. <https://doi.org/10.1111/ecog.00802>
- Damschen, E. I., Harrison, S., & Grace, J. B. (2010). *Climate change effects on an endemic-rich edaphic flora: Resurveying Robert H. Whittaker's Siskiyou sites (Oregon, USA)*. <https://pubag.nal.usda.gov/catalog/5712174>
- Davis, E. J., Huber-Stearns, H., Cheng, A. S., & Jacobson, M. (2021). Transcending Parallel Play: Boundary Spanning for Collective Action in Wildfire Management. *Fire*, 4(3), 41. <https://doi.org/10.3390/fire4030041>
- D'Evelyn, S. M., Jung, J., Alvarado, E., Baumgartner, J., Caligiuri, P., Hagmann, R. K., Henderson, S. B., Hessburg, P. F., Hopkins, S., Kasner, E. J., Krawchuk, M. A., Krenz, J. E., Lydersen, J. M., Marlier, M. E., Masuda, Y. J., Metlen, K., Mittelstaedt, G., Prichard, S. J., Schollaert, C. L., ... Spector, J. T. (2022). Wildfire, Smoke Exposure, Human Health, and Environmental Justice Need to be Integrated into Forest Restoration and Management. *Current Environmental Health Reports*. <https://doi.org/10.1007/s40572-022-00355-7>
- Donato, D. C., Fontaine, J. B., Campbell, J. L., Robinson, W. D., Kauffman, J. B., & Law, B. E. (2009). Conifer regeneration in stand-replacement portions of a large mixed-severity wildfire in the Klamath–Siskiyou Mountains. *Canadian Journal of Forest Research*, 39(4), 823–838. <https://doi.org/10.1139/X09-016>

- Dunn, C. J., O'Connor, C. D., Abrams, J., Thompson, M. P., Calkin, D. E., Johnston, J. D., Stratton, R., & Gilbertson-Day, J. (2020). Wildfire risk science facilitates adaptation of fire-prone social-ecological systems to the new fire reality. *Environmental Research Letters*, *15*(2), 025001. <https://doi.org/10.1088/1748-9326/ab6498>
- Duveneck, M. J., Scheller, R. M., White, M. A., Handler, S. D., & Ravenscroft, C. (2014). Climate change effects on northern Great Lake (USA) forests: A case for preserving diversity. *Ecosphere*, *5*(2), art23. <https://doi.org/10.1890/ES13-00370.1>
- Eidenshink, J., Schwind, B., Brewer, K., Zhu, Z.-L., Quayle, B., & Howard, S. (2007). A Project for Monitoring Trends in Burn Severity. *Fire Ecology*, *3*(1), 3–21. <https://doi.org/10.4996/fireecology.0301003>
- Fernandes, P. M. (2015). Empirical Support for the Use of Prescribed Burning as a Fuel Treatment. *Current Forestry Reports*, *1*(2), 118–127. <https://doi.org/10.1007/s40725-015-0010-z>
- Friesen, C. A. (1991). *The effect of broadcast burning on the quality of winter forage for Elk, Western Oregon*. [Thesis]. Oregon State University.
- Griffith, G. E., Omernik, J. M., Smith, D. W., Cook, T. D., Tallyn, E., Moseley, K., & Johnson, C. B. (2016). *Ecoregions of California* [Poster]. US Geological Survey. <http://dx.doi.org/10.3133/ofr20161021>
- Griscom, B. W., Adams, J., Ellis, P. W., Houghton, R. A., Lomax, G., Miteva, D. A., Schlesinger, W. H., Shoch, D., Sükamäki, J. V., Smith, P., Woodbury, P., Zganjar, C., Blackman, A., Campari, J., Conant, R. T., Delgado, C., Elias, P., Gopalakrishna, T., Hamsik, M. R., ... Fargione, J. (2017). Natural climate solutions. *Proceedings of the National Academy of Sciences*, *114*(44), 11645–11650. <https://doi.org/10.1073/pnas.1710465114>
- Gustafson, E. J., Shifley, S. R., Mladenoff, D. J., Nimerfro, K. K., & He, H. S. (2000). Spatial simulation of forest succession and timber harvesting using LANDIS. *Canadian Journal of Forest Research*, *30*(1), 32–43. <https://doi.org/10.1139/x99-188>
- Halofsky, J. E., Donato, D. C., Hibbs, D. E., Campbell, J. L., Cannon, M. D., Fontaine, J. B., Thompson, J. R., Anthony, R. G., Bormann, B. T., Kayes, L. J., Law, B. E., Peterson, D. L., & Spies, T. A. (2011). Mixed-severity fire regimes: Lessons and hypotheses from the Klamath-Siskiyou Ecoregion. *Ecosphere*, *2*(4), art40. <https://doi.org/10.1890/ES10-00184.1>
- Haugo, R. D., Kellogg, B. S., Cansler, C. A., Kolden, C. A., Kemp, K. B., Robertson, J. C., Metlen, K. L., Vaillant, N. M., & Restaino, C. M. (2019). The missing fire: Quantifying human exclusion of wildfire in Pacific Northwest forests. *Ecosphere*, *10*(4), e02702. <https://doi.org/10.1002/ecs2.2702>
- Hijman, R. (2022). *terra: Spatial Data Analysis* (1.5-34) [R]. <https://CRAN.R-project.org/package=terra>

- Hood, S., & Lutes, D. (2017). Predicting Post-Fire Tree Mortality for 12 Western US Conifers Using the First Order Fire Effects Model (FOFEM). *Fire Ecology*, 13(2), 66–84. <https://doi.org/10.4996/fireecology.130290243>
- Hudiburg, T., Law, B., Turner, D. P., Campbell, J., Donato, D., & Duane, M. (2009). Carbon dynamics of Oregon and Northern California forests and potential land-based carbon storage. *Ecological Applications*, 19(1), 163–180. <https://doi.org/10.1890/07-2006.1>
- Huff, S., Poudel, K. P., Ritchie, M., & Temesgen, H. (2018). Quantifying aboveground biomass for common shrubs in northeastern California using nonlinear mixed effect models. *Forest Ecology and Management*, 424, 154–163. <https://doi.org/10.1016/j.foreco.2018.04.043>
- Hurteau, M. D., & Brooks, M. L. (2011). Short- and Long-term Effects of Fire on Carbon in US Dry Temperate Forest Systems. *BioScience*, 61(2), 139–146. <https://doi.org/10.1525/bio.2011.61.2.9>
- Hurteau, M. D., North, M. P., Koch, G. W., & Hungate, B. A. (2019). Opinion: Managing for disturbance stabilizes forest carbon. *Proceedings of the National Academy of Sciences*, 116(21), 10193–10195. <https://doi.org/10.1073/pnas.1905146116>
- Hurt, G. C., Pacala, S. W., Moorcroft, P. R., Caspersen, J., Shevliakova, E., Houghton, R. A., & Moore, B. (2002). Projecting the future of the U.S. carbon sink. *Proceedings of the National Academy of Sciences*, 99(3), 1389–1394. <https://doi.org/10.1073/pnas.012249999>
- Iversen, C. M., McCormack, M. L., Baer, J. K., Powell, A. S., Chen, W., Collins, C., Fan, Y., Fanin, N., Freschet, G. T., Guo, D., Hogan, J. A., Kou, L., Laughlin, D. C., Lavelly, E., Liese, R., Lin, D., Meier, I. C., Montagnoli, A., Roumet, C., ... Zadworny, M. (2021). *Fine-Root Ecology Database (FRED): A Global Collection of Root Trait Data with Coincident Site, Vegetation, Edaphic, and Climatic Data, Version 3*. Oak Ridge National Laboratory, TES SFA, US Department of Energy. <https://doi.org/10.25581/ornlsfa.014/1459186>
- Kalies, E. L., & Kent, L. L. Y. (2016). Tamm Review: Are fuel treatments effective at achieving ecological and social objectives? A systematic review. *Forest Ecology and Management*, 375, 84–95. <https://doi.org/10.1016/j.foreco.2016.05.021>
- Kassambara, A. (2020). *ggpubr: “ggplot2” based publication ready plots* (0.4.0) [R]. <https://CRAN.R-project.org/package=ggpubr>
- Kattge, J., Bönsch, G., Díaz, S., Lavorel, S., Prentice, I. C., Leadley, P., Tautenhahn, S., Werner, G. D. A., Aakala, T., Abedi, M., Acosta, A. T. R., Adamidis, G. C., Adamson, K., Aiba, M., Albert, C. H., Alcántara, J. M., Alcázar, C. C., Aleixo, I., Ali, H., ... Wirth, C. (2020). TRY plant trait database – enhanced coverage and open access. *Global Change Biology*, 26(1), 119–188. <https://doi.org/10.1111/gcb.14904>
- Keyser, C. (2019). *Inland California and Southern Cascades (CA) Variant Overview—Forest Vegetation Simulator* (p. 79). USDA Forest Service, Forest Management Service Center.

- Kimmerer, R. W., & Lake, F. K. (2001). The Role of Indigenous Burning in Land Management. *Journal of Forestry*, 99(11), 36–41. <https://doi.org/10.1093/jof/99.11.36>
- Knight, C., Anderson, L., Champagne, M., Clayburn, R. M., Crawford, J. N., Klimaszewski-Patterson, A., Knapp, E. E., Lake, F. K., Mensing, S. A., Wahl, D., Wanker, J., Watts-Tobin, A., Potts, M. D., & Battles, J. J. (2022). Land management explains major trends in forest structure and composition over the last millennium in California's Klamath Mountains. *PNAS*, 119(12), e2116264119. <https://doi.org/10.1073/pnas.2116264119>
- Kolden, C. A. (2019). We're Not Doing Enough Prescribed Fire in the Western United States to Mitigate Wildfire Risk. *Fire*, 2(2), 30. <https://doi.org/10.3390/fire2020030>
- Lake, F. K. (2021). Indigenous Fire Stewardship: Federal/Tribal Partnerships for Wildland Fire Research and Management. *Fire Management Today*, 79(1), 30–39.
- Lake, F. K., Wright, V., Morgan, P., McFadzen, M., McWethy, D., & Stevens-Rumann, C. (2017). Returning Fire to the Land: Celebrating Traditional Knowledge and Fire. *Journal of Forestry*, 115(5), 343–353. <https://doi.org/10.5849/jof.2016-043R2>
- LaLande, J., & Pullen, R. (1999). Burning for a “Fine and Beautiful Open Country”: Native Uses of Fire in Southwestern Oregon. In R. Boyd (Ed.), *Indians, Fire, and the Land in the Pacific Northwest* (pp. 225–276). Oregon State University Press.
- LANDFIRE. (2014). *Fuel characteristics classification system fuelbeds* [US Geological Survey & US Forest Service]. <http://landfire.cr.usgs.gov/viewer/>
- Levy, S. (2022). The Return of Intentional Forest Fires: Scientists look to Indigenous practices. *BioScience*, biac016. <https://doi.org/10.1093/biosci/biac016>
- Lewis, H. T. (1973). *Patterns of Indian Burning in California: Ecology and Ethnobotany*. Ballena Press.
- Liang, S., Hurteau, M. D., & Westerling, A. L. (2018). Large-scale restoration increases carbon stability under projected climate and wildfire regimes. *Frontiers in Ecology and the Environment*, 16(4), 207–212. <https://doi.org/10.1002/fee.1791>
- Long, J. W., Gray, A., & Lake, F. K. (2018). Recent Trends in Large Hardwoods in the Pacific Northwest, USA. *Forests*, 9(10), 651. <https://doi.org/10.3390/f9100651>
- Loudermilk, E. L., Stanton, A., Scheller, R. M., Dilts, T. E., Weisberg, P. J., Skinner, C., & Yang, J. (2014). Effectiveness of fuel treatments for mitigating wildfire risk and sequestering forest carbon: A case study in the Lake Tahoe Basin. *Forest Ecology and Management*, 323, 114–125. <https://doi.org/10.1016/j.foreco.2014.03.011>
- Lucash, M. S., Scheller, R. M., Sturtevant, B. R., Gustafson, E. J., Kretchun, A. M., & Foster, J. R. (2018). More than the sum of its parts: How disturbance interactions shape forest dynamics under climate change. *Ecosphere*, 9(6), e02293. <https://doi.org/10.1002/ecs2.2293>

- Marks-Block, T., & Tripp, W. (2021). Facilitating Prescribed Fire in Northern California through Indigenous Governance and Interagency Partnerships. *Fire*, 4(3), 37. <https://doi.org/10.3390/fire4030037>
- Marlon, J. R., Bartlein, P. J., Gavin, D. G., Long, C. J., Anderson, R. S., Briles, C. E., Brown, K. J., Colombaroli, D., Hallett, D. J., Power, M. J., Scharf, E. A., & Walsh, M. K. (2012). Long-term perspective on wildfires in the western USA. *Proceedings of the National Academy of Sciences*, 109(9), E535–E543. <https://doi.org/10.1073/pnas.1112839109>
- Maxwell, C. J., Serra-Diaz, J. M., Scheller, R. M., & Thompson, J. R. (2020). Co-designed management scenarios shape the responses of seasonally dry forests to changing climate and fire regimes. *Journal of Applied Ecology*, 57(7), 1328–1340. <https://doi.org/10.1111/1365-2664.13630>
- Meerdink, S. K., Roberts, D. A., King, J. Y., Roth, K. L., Dennison, P. E., Amaral, C. H., & Hook, S. J. (2016). Linking seasonal foliar traits to VSWIR-TIR spectroscopy across California ecosystems. *Remote Sensing of Environment*, 186, 322–338. <https://doi.org/10.1016/j.rse.2016.08.003>
- Metlen, K. L., Skinner, C. N., Olson, D. R., Nichols, C., & Borgias, D. (2018). Regional and local controls on historical fire regimes of dry forests and woodlands in the Rogue River Basin, Oregon, USA. *Forest Ecology and Management*, 430, 43–58. <https://doi.org/10.1016/j.foreco.2018.07.010>
- Mladenoff, D. J. (2004). LANDIS and forest landscape models. *Ecological Modelling*, 180(1), 7–19. <https://doi.org/10.1016/j.ecolmodel.2004.03.016>
- Mu, Q., Zhao, M., & Running, S. W. (2013). *MODIS Global Terrestrial Evapotranspiration (ET) Product (NASA MOD16A2/A3) Algorithm Theoretical Basis Document Collection 5*. Numerical Terradynamic Simulation Group, College of Forestry and Conservation, The University of Montana.
- Myneni, Y. K. R., & Park, T. (2015). MOD15A2H MODIS/Terra Leaf Area Index/FPAR 8-Day L4 Global 500m SIN Grid V006. *NASA EOSDIS Land Processes DAAC*. <https://doi.org/10.5067/MODIS/MOD15A2H.006>
- National Centers for Environmental Information [NCEI]. (2020). *Gridded NCEI Normals Mapper*. <https://www.ncei.noaa.gov/products/land-based-station/us-climate-normals>
- Neill, A. R., & Puettmann, K. J. (2013). Managing for adaptive capacity: Thinning improves food availability for wildlife and insect pollinators under climate change conditions. *Canadian Journal of Forest Research*, 43(5), 428–440. <https://doi.org/10.1139/cjfr-2012-0345>
- NEON (National Ecological Observatory Network). (2021). *Plant foliar traits (DP1.10026.001)*. <https://doi.org/10.48443/kmc7-8g05>

- Neuenschwander, A., Guenther, E., White, J. C., Duncanson, L., & Montesano, P. (2020). Validation of ICESat-2 terrain and canopy heights in boreal forests. *Remote Sensing of Environment*, 251, 112110. <https://doi.org/10.1016/j.rse.2020.112110>
- Neuenschwander, A. L., & Magruder, L. A. (2019). Canopy and Terrain Height Retrievals with ICESat-2: A First Look. *Remote Sensing*, 11(14), 1721. <https://doi.org/10.3390/rs11141721>
- Neumann, T. A., Brenner, A., Hancock, D., Robbins, J., Saba, J., Harbeck, K., Gibbons, A., Lee, J., Luthke, S. B., Rebold, T., & et al. (2021). ATLAS/ICESat-2 L2A Global Geolocated Photon Data, Version 4. [ATL03]. *NASA National Snow and Ice Data Center Distributed Active Archive Center*. <https://doi.org/10.5067/ATLAS/ATL03.004>.
- Nixon, K. C. (2002). The oak (*Quercus*) biodiversity of California and adjacent regions. In R. B. Standiford (Ed.), *Proceedings of the Fifth Symposium on Oak Woodlands: Oaks in California's Challenging Landscape* (pp. 3–20). Pacific Southwest Research Station, Forest Service, US Department of Agriculture. <http://www.fs.usda.gov/treearch/pubs/26105>
- North, M. P., York, R. A., Collins, B. M., Hurteau, M. D., Jones, G. M., Knapp, E. E., Kobziar, L., McCann, H., Meyer, M. D., Stephens, S. L., Tompkins, R. E., & Tubbesing, C. L. (2021). Pyrosilviculture Needed for Landscape Resilience of Dry Western United States Forests. *Journal of Forestry*, 119(5), 520–544. <https://doi.org/10.1093/jofore/fvab026>
- Ohmann, J. L., & Gregory, M. J. (2002). Predictive mapping of forest composition and structure with direct gradient analysis and nearest- neighbor imputation in coastal Oregon, U.S.A. *Canadian Journal of Forest Research*, 32(4), 725–741. <https://doi.org/10.1139/x02-011>
- ORNL DAAC. (2018). *MODIS and VIIRS land products global subsetting and visualization tool*. <https://doi.org/10.3334/ORNLDAAC/1379>
- Parks, S. A., & Abatzoglou, J. T. (2020). Warmer and Drier Fire Seasons Contribute to Increases in Area Burned at High Severity in Western US Forests From 1985 to 2017. *Geophysical Research Letters*, 47(22), e2020GL089858. <https://doi.org/10.1029/2020GL089858>
- Parton, W. J., Schimel, D. S., Cole, C. V., & Ojima, D. S. (1987). Analysis of Factors Controlling Soil Organic Matter Levels in Great Plains Grasslands. *Soil Science Society of America Journal*, 51(5), 1173–1179. <https://doi.org/10.2136/sssaj1987.03615995005100050015x>
- Parton, W. J., Stewart, J. W. B., & Cole, C. V. (1988). Dynamics of C, N, P and S in grassland soils: A model. *Biogeochemistry*, 5(1), 109–131. <https://doi.org/10.1007/BF02180320>
- Pellegrini, A. F. A., Ahlström, A., Hobbie, S. E., Reich, P. B., Nieradzik, L. P., Staver, A. C., Scharenbroch, B. C., Jumpponen, A., Anderegg, W. R. L., Randerson, J. T., & Jackson, R. B. (2018). Fire frequency drives decadal changes in soil carbon and nitrogen and ecosystem productivity. *Nature*, 553(7687), 194–198. <https://doi.org/10.1038/nature24668>

- Perry, D. A., Hessburg, P. F., Skinner, C. N., Spies, T. A., Stephens, S. L., Taylor, A. H., Franklin, J. F., McComb, B., & Riegel, G. (2011). The ecology of mixed severity fire regimes in Washington, Oregon, and Northern California. *Forest Ecology and Management*, 262(5), 703–717. <https://doi.org/10.1016/j.foreco.2011.05.004>
- PRISM Climate Group. (2021). *United States Average Annual Total Precipitation, 1991-2020*. Oregon State University. prism.oregonstate.edu
- Pyne, S. J. (1997). *Fire in America: A Cultural History of Wildland and Rural Fire*. University of Washington Press.
- R Core Team. (2022). *R: A Language and Environment for Statistical Computing* (4.2.0). R Foundation for Statistical Computing.
- Restaino, J. C., & Peterson, D. L. (2013). Wildfire and fuel treatment effects on forest carbon dynamics in the western United States. *Forest Ecology and Management*, 303, 46–60. <https://doi.org/10.1016/j.foreco.2013.03.043>
- Riccardi, C. L., Prichard, S. J., Sandberg, D. V., & Ottmar, R. D. (2007). Quantifying physical characteristics of wildland fuels using the fuel characteristic classification system. *Canadian Journal of Forestry Research*, 37, 2413–2420. <https://doi.org/10.1139/X07-175>
- RStudio Team. (2022). *RStudio: Integrated Development Environment for R* (2022.02.03). RStudio, PBC. <http://www.rstudio.com/>
- Rundel, P. W. (1979). *Adaptations of Mediterranean Oaks to Environmental Stress*. the Symposium on the Ecology, Management, and Utilization of California Oaks, Claremont, CA.
- Rupp, D. E., Abatzoglou, J. T., Hegewisch, K. C., & Mote, P. W. (2013). Evaluation of CMIP5 20th century climate simulations for the Pacific Northwest USA. *Journal of Geophysical Research: Atmospheres*, 118(19), 10,884–10,906. <https://doi.org/10.1002/jgrd.50843>
- Scheller, R., Kretchun, A., Hawbaker, T. J., & Henne, P. D. (2019). A landscape model of variable social-ecological fire regimes. *Ecological Modelling*, 401, 85–93. <https://doi.org/10.1016/j.ecolmodel.2019.03.022>
- Scheller, R. M., Domingo, J. B., Sturtevant, B. R., Williams, J. S., Rudy, A., Gustafson, E. J., & Mladenoff, D. J. (2007). Design, development, and application of LANDIS-II, a spatial landscape simulation model with flexible temporal and spatial resolution. *Ecological Modelling*, 201(3), 409–419. <https://doi.org/10.1016/j.ecolmodel.2006.10.009>
- Scheller, R. M., Hua, D., Bolstad, P. V., Birdsey, R. A., & Mladenoff, D. J. (2011). The effects of forest harvest intensity in combination with wind disturbance on carbon dynamics in Lake States Mesic Forests. *Ecological Modelling*, 222(1), 144–153. <https://doi.org/10.1016/j.ecolmodel.2010.09.009>

- Scheller, R. M., & Mladenoff, D. J. (2004). A forest growth and biomass module for a landscape simulation model, LANDIS: Design, validation, and application. *Ecological Modelling*, *180*(1), 211–229. <https://doi.org/10.1016/j.ecolmodel.2004.01.022>
- Scheller, R. M., Van Tuyl, S., Clark, K. L., Hom, J., & La Puma, I. (2011). Carbon Sequestration in the New Jersey Pine Barrens Under Different Scenarios of Fire Management. *Ecosystems*, *14*(6), 987–1004. <https://doi.org/10.1007/s10021-011-9462-6>
- Schoennagel, T., Veblen, T. T., & Romme, W. H. (2004). The Interaction of Fire, Fuels, and Climate across Rocky Mountain Forests. *BioScience*, *54*(7), 661–676. [https://doi.org/10.1641/0006-3568\(2004\)054\[0661:TIOFFA\]2.0.CO;2](https://doi.org/10.1641/0006-3568(2004)054[0661:TIOFFA]2.0.CO;2)
- Schultz, C. A., McCaffrey, S. M., Huber-Stearns, H. R., Schultz, C. A., McCaffrey, S. M., & Huber-Stearns, H. R. (2019). Policy barriers and opportunities for prescribed fire application in the western United States. *International Journal of Wildland Fire*, *28*(11), 874–884. <https://doi.org/10.1071/WF19040>
- Schwarz, G. E., & Alexander, R. B. (1995). *Soils data for the Conterminous United States Derived from the NRCS State Soil Geographic (STATSGO) Data Base*. US Geological Survey. <https://water.usgs.gov/lookup/getspatial?ussoils>
- Sensenig, T., Bailey, J. D., & Tappeiner, J. C. (2013). Stand development, fire and growth of old-growth and young forests in southwestern Oregon, USA. *Forest Ecology and Management*, *291*, 96–109. <https://doi.org/10.1016/j.foreco.2012.11.006>
- Serra-Diaz, J. M., Maxwell, C., Lucash, M. S., Scheller, R. M., Laflower, D. M., Miller, A. D., Tepley, A. J., Epstein, H. E., Anderson-Teixeira, K. J., & Thompson, J. R. (2018). Disequilibrium of fire-prone forests sets the stage for a rapid decline in conifer dominance during the 21 st century. *Scientific Reports*, *8*(1), 6749. <https://doi.org/10.1038/s41598-018-24642-2>
- Short, K. (2021). Spatial wildfire occurrence data for the United States, 1992-2018 [FPA_FOD_20210617]. *Forest Service Research Data Archive*. <https://doi.org/10.2737/RDS-2013-0009.5>
- Silva, L. C. R., Wood, M. C., Johnson, B. R., Coughlan, M. R., Brinton, H., McGuire, K., & Bridgham, S. D. (2022). A generalizable framework for enhanced natural climate solutions. *Plant and Soil*. <https://doi.org/10.1007/s11104-022-05472-8>
- Smithwick, E. A. H., Harmon, M. E., Remillard, S. M., Acker, S. A., & Franklin, J. F. (2002). Potential Upper Bounds of Carbon Stores in Forests of the Pacific Northwest. *Ecological Applications*, *12*(5), 1303–1317. [https://doi.org/10.1890/1051-0761\(2002\)012\[1303:PUBOCS\]2.0.CO;2](https://doi.org/10.1890/1051-0761(2002)012[1303:PUBOCS]2.0.CO;2)
- Stephens, S. L., Westerling, A. L., Hurteau, M. D., Peery, M. Z., Schultz, C. A., & Thompson, S. (2020). Fire and climate change: Conserving seasonally dry forests is still possible. *Frontiers in Ecology and the Environment*, *18*(6), 354–360. <https://doi.org/10.1002/fee.2218>

- Syphard, A. D., Scheller, R. M., Ward, B. C., Spencer, W. D., Strittholt, J. R., Syphard, A. D., Scheller, R. M., Ward, B. C., Spencer, W. D., & Strittholt, J. R. (2011). Simulating landscape-scale effects of fuels treatments in the Sierra Nevada, California, USA. *International Journal of Wildland Fire*, 20(3), 364–383. <https://doi.org/10.1071/WF09125>
- Taylor, A. H., Harris, L. B., & Drury, S. A. (2021). Drivers of fire severity shift as landscapes transition to an active fire regime, Klamath Mountains, USA. *Ecosphere*, 12(9), e03734. <https://doi.org/10.1002/ecs2.3734>
- Taylor, A. H., & Skinner, C. N. (2003). Spatial Patterns and Controls on Historical Fire Regimes and Forest Structure in the Klamath Mountains. *Ecological Applications*, 13(3), 704–719. [https://doi.org/10.1890/1051-0761\(2003\)013\[0704:SPACOH\]2.0.CO;2](https://doi.org/10.1890/1051-0761(2003)013[0704:SPACOH]2.0.CO;2)
- Taylor, K. E., Stouffer, R. J., & Meehl, G. A. (2012). An Overview of CMIP5 and the Experiment Design. *Bulletin of the American Meteorological Society*, 93(4), 485–498. <https://doi.org/10.1175/BAMS-D-11-00094.1>
- Tepley, A. J., Thompson, J. R., Epstein, H. E., & Anderson-Teixeira, K. J. (2017). Vulnerability to forest loss through altered postfire recovery dynamics in a warming climate in the Klamath Mountains. *Global Change Biology*, 23(10), 4117–4132. <https://doi.org/10.1111/gcb.13704>
- Thompson, R. S., Anderson, K. H., Pelltier, R. T., Strickland, L. E., Shafer, S. L., Bartlein, P. J., & McFadden, A. K. (2015). *Atlas of relations between climatic parameters and distributions of important trees and shrubs in North America- Revisions for all taxa from the United States and Canada and new taxa from the western United States* (USGS Professional Paper No. 1650-G). US Geological Survey. <http://dx.doi.org/10.3133/pp1650G>
- Thompson, R. S., Anderson, K. H., Strickland, L. E., Shafer, S. L., Pelltier, R. T., & Bartlein, P. J. (2006). *Atlas of relations between climatic parameters and distributions of important trees and shrubs in North America- Revisions for all taxa from the United States and Canada and new taxa from the western United States* (USGS Professional Paper No. 1650; p. 342). US Geological Survey. <http://dx.doi.org/10.3133/pp1650G>.
- Turner, M. G., Donato, D. C., & Romme, W. H. (2013). Consequences of spatial heterogeneity for ecosystem services in changing forest landscapes: Priorities for future research. *Landscape Ecology*, 28(6), 1081–1097. <https://doi.org/10.1007/s10980-012-9741-4>
- US Geological Survey. (2020). *1 Arc-second Digital Elevation Models (DEMs)—USGS National Map 3DEP Downloadable Data Collection*. <https://nationalmap.gov/3DEP/>
- US Geological Survey [USGS]. (2020). *1/3rd arc-second Digital Elevation Models (DEMs)—USGS National Map 3DEP Downloadable Data Collection*. <https://data.usgs.gov/datacatalog/data/USGS:3a81321b-c153-416f-98b7-cc8e5f0e17c3>
- USDA Forest Service. (2015). *The Rising Cost of Wildfire Operations*. 17.

- USDA Forest Service. (2022). *Confronting the Wildfire Crisis: A 10-year Implementation Plan* (FS-1187b; p. 20). USDA Forest Service. <https://www.fs.usda.gov/sites/default/files/Wildfire-Crisis-Implementation-Plan.pdf>
- USDA Forest Service & US Geological Survey. (2021a). *Monitoring Trends in Burn Severity Burned Areas Boundaries for 1984-2019*. <https://mtbs.gov/direct-download>
- USDA Forest Service & US Geological Survey. (2021b). *Monitoring Trends in Burn Severity Fire Occurrence Dataset (FOD) Point Locations from 1984-2019*. <https://doi.org/10.5066/P9IED7RZ>
- USFS. (2022). *Forest Inventory and Analysis Database*. <http://apps.fs.fed.us/fiadb-downloads/datamart.html>
- USGS. (2021). *NFPORS Hazardous Fuels Reduction Treatment Units*. USGS Geosciences and Environmental Science Center. https://usgs.nfpors.gov/arcgis/rest/services/nfpors_treats/MapServer.
- Vaillant, N. M., & Reinhardt, E. D. (2017). An Evaluation of the Forest Service Hazardous Fuels Treatment Program—Are We Treating Enough to Promote Resiliency or Reduce Hazard? *Journal of Forestry*, 115(4), 300–308. <https://doi.org/10.5849/jof.16-067>
- Walkinshaw, M., O'Green, A. T., & Beaudette, D. E. (2020). *Soil Properties*. California Soil Resource Lab. <https://casoilresource.lawr.ucdavis.edu/soil-properties/>
- West, T. O. (2014). *Soil Carbon Estimates in 20-cm Layers to 1-meter Depth, Conterminous US, 1970-1993*. Oak Ridge National Laboratory Distributed Active Archive Center for Biogeochemical Dynamics. <https://doi.org/10.3334/ORNLDAAAC/1238>
- Whittaker, R. H. (1960). Vegetation of the Siskiyou Mountains, Oregon and California. *Ecological Monographs*, 30(3), 61. <https://doi.org/10.2307/1943563>
- Wickham, H. (2016). *ggplot2: Elegant Graphics for Data Analysis*. Springer-Verlog.
- Wickham, H., Francois R., Henry, L., & Muller, K. (2022). *dplyr: A Grammar of Data Manipulation*. (1.0.9) [R]. <https://CRAN.R-project.org/package=dplyr>
- Wilson, B. T., Woodall, C. W., & Griffith, D. M. (2013). *Forest carbon stocks of the contiguous United States (2000-2009)*. US Forest Service. <https://doi.org/10.2737/RDS-2013-0004>
- Woodall, C. W., Heath, L. S., Domke, G. M., & Nichols, M. C. (2010). Methods and equations for estimating aboveground volume, biomass, and carbon for trees in the U.S. forest inventory, 2010. *USDA Forest Service Northern Research Station, General Technical Report NRS-88*, 30. <https://doi.org/10.2737/NRS-GTR-88>.

- Yan, K., Park, T., Yan, G., Liu, Z., Yang, B., Chen, C., Nemani, R. R., Knyazikhin, Y., & Myneni, R. B. (2016). Evaluation of MODIS LAI/FPAR Product Collection 6. Part 2: Validation and Intercomparison. *Remote Sensing*, *8*(6), 460. <https://doi.org/10.3390/rs8060460>
- Zhang, J., Tian, J., Li, X., Wang, L., Chen, B., Gong, H., Ni, R., Zhou, B., & Yang, C. (2021). Leaf area index retrieval with ICESat-2 photon counting LiDAR. *International Journal of Applied Earth Observation and Geoinformation*, *103*, 102488. <https://doi.org/10.1016/j.jag.2021.102488>
- Zhou, Y., Singh, J., Butnor, J. R., Coetsee, C., Boucher, P. B., Case, M. F., Hockridge, E. G., Davies, A. B., & Staver, A. C. (2022). Limited increases in savanna carbon stocks over decades of fire suppression | Nature. *Nature*, *603*, 445–449. <https://doi.org/10.1038/s41586-022-04438-1>